

# Modelling of pressure waves in the Common Rail Diesel Injection System

**Kristina Ahlin**

LiTH-ISY-EX-3081

December 11, 2000



# **Modelling of pressure waves in the Common Rail Diesel Injection System**

Examensarbete utfört i Fordonssystem  
vid Tekniska Högskolan i Linköping  
av

**Kristina Ahlin**


Reg nr: LiTH-ISY-EX-3081

Supervisor: **Michael Froehlich, Daimler Chrysler  
AG  
Dr Lars Eriksson, Fordonssystem  
Lith**

Examiner: **Prof. Lars Nielsen**

Linköping, December 11, 2000.



	<b>Avdelning, Institution</b> Division, Department Vehicular Systems Dept. of Electrical Engineering	<b>Datum:</b> Date: December 11, 2000
	<b>Språk</b> Language <input type="checkbox"/> Svenska/Swedish <input checked="" type="checkbox"/> Engelska/English <input type="checkbox"/> _____	<b>Rapporttyp</b> Report category <input type="checkbox"/> Licentiatavhandling <input checked="" type="checkbox"/> Examensarbete <input type="checkbox"/> C-uppsats <input type="checkbox"/> D-uppsats <input type="checkbox"/> Övrig rapport <input type="checkbox"/> _____
<b>URL för elektronisk version</b> <a href="http://www.fs.isy.liu.se">http://www.fs.isy.liu.se</a>		
<b>Titel:</b> Modellering av tryckvågor i Common Rail Diesel Injection System <b>Title:</b> Modelling of pressure waves in the Common Rail Diesel Injection System  <b>Författare:</b> Kristina Ahlin <b>Author:</b>		
<b>Sammanfattning</b> Abstract <p>The aim of this study is to describe the behaviour of the pressure in the Common Rail Diesel Injection System mathematically. In order to understand the wave phenomena that may occur in the system, a physical model is desired. The model will be used for examining the cause of problems in the OM613 Common Rail Diesel Injection Engine that arise at certain critical working conditions. Another object of a model of the system is to use it together with a model of the injector for diagnosis purposes.</p> <p>Two different modelling methods are used and both models are based on well known physical relations. The first approach implies that the pressure waves are approximated with mechanical waves in a mass spring system. The model developed by this method does not describe the measured data very well, which mainly depend on too inaccurate estimations of physical parameters. The second method is developed from the general wave equation. This model describes the system more strictly and presents accordingly much better results than the first model. For the above explained purposes the latter model is recommended. Simulations show satisfactory results but improvements are naturally possible.</p> <p>Since the models are developed for a certain working point they can not be expected to be valid for all working conditions. When the physical parameters for the critical working point becomes clear, a new model can be generated out of the first one by only correcting a few constants.</p>		
<b>Nyckelord</b> Common Rail Diesel Injection System, physical modelling, superposition of <b>Keywords</b> waves, wave equation, partial differential equation		



## Abstract

The aim of this study is to describe the behaviour of the pressure in the Common Rail Diesel Injection System mathematically. In order to understand the wave phenomena that may occur in the system, a physical model is desired. The model will be used for examining the cause of problems in the OM613 Common Rail Diesel Injection Engine that arise at certain critical working conditions. Another object of a model of the system is to use it together with a model of the injector for diagnosis purposes.

Two different modelling methods are used and both models are based on well known physical relations. The first approach implies that the pressure waves are approximated with mechanical waves in a mass spring system. The model developed by this method does not describe the measured data very well, which mainly depend on too inaccurate estimations of physical parameters. The second method is developed from the general wave equation. This model describes the system more strictly and presents accordingly much better results than the first model. For the above explained purposes the latter model is recommended. Simulations show satisfactory results but improvements are naturally possible.

Since the models are developed for a certain working point they can not be expected to be valid for all working conditions. When the physical parameters for the critical working point becomes clear, a new model can be generated out of the first one by only correcting a few constants.

**Key words:** Common Rail Diesel Injection System, physical modelling, superposition of waves, wave equation, partial differential equation

## Acknowledgments

This work is carried out in the engine control team at Daimler Chrysler AG in Stuttgart. I would like to thank everyone who has helped me during the work.

Stuttgart, November 2000

Kristina Ahlin

## Notation

### General Symbols

$K$	compressibility constant
$\rho$	density
$p$	pressure
$p_0$	equilibrium pressure
$x_i(t)$	state variable
$\dot{x}_i(t)$	time derivative of the state variable
$u_i(t)$	input signal
$y_i(t)$	output signal
$\xi(t)$	displacement from an equilibrium position
$f_{ri}$	frequencies of possible standing waves in the rail
$f_{pi}$	frequencies of possible standing waves in the pump pipe
$f_{ii}$	frequencies of possible standing waves in the injection pipes
$v$	speed of the wave
$k$	harmonic number
$l_r$	length of the rail
$\lambda_{ri}$	wave length of the possible standing waves in the rail
$L$	inductance
$C$	capacitance
$R$	resistance
$i(t)$	current
$u(t)$	voltage
$v(t)$	velocity
$V$	volume
$A$	cross section area

### Symbols used in the mass spring model

$c$	damping constant
$F(t)$	force
$A_{inj}$	cross section area of the injector pipe
$A_{rail}$	cross section area of the rail
$V_{rail}$	volume of the rail
$l$	length of an uneffected spring
$k$	spring constant
$m$	mass



**Symbols used in the wave equation model**

$\eta$	dynamic viscosity
$c$	speed of the wave
$s$	condensation
$R$	damping constant

**Abbreviations**

CR	Common Rail
CDI	Common Rail Diesel Injection
ECU	Engine Control Unit
DI	Direct Injection
IDI	Indirect Injection

## Contents

<b>1</b>	<b>Introduction</b>	<b>1</b>
1.1	Background . . . . .	1
1.2	The thesis . . . . .	1
1.3	Methods . . . . .	1
1.4	Thesis Outline . . . . .	2
<b>2</b>	<b>The Common Rail Diesel Injection System</b>	<b>3</b>
2.1	Injection systems . . . . .	3
2.2	The high pressure circuit . . . . .	4
2.3	The low pressure circuit . . . . .	5
2.4	The ECU with sensors . . . . .	5
<b>3</b>	<b>The Common Rail Diesel Injection System from a modelling point of view</b>	<b>6</b>
3.1	The aim of the model and the desired properties . . . . .	6
3.2	Measured signals used in the model . . . . .	6
3.2.1	The pump . . . . .	7
3.2.2	The pressure control valve . . . . .	8
3.2.3	The injectors . . . . .	9
3.3	Frequency analysis . . . . .	12
3.3.1	The pump signal . . . . .	13
3.3.2	The rail signal . . . . .	16
3.3.3	Other working points . . . . .	17
<b>4</b>	<b>The Mass spring method</b>	<b>19</b>
4.1	The model . . . . .	19
4.1.1	The basic equation . . . . .	19
4.1.2	Bondgraphs . . . . .	20
4.1.3	The Bondgraph method applied to the CR System . . . . .	24
4.1.4	Boundary conditions . . . . .	25
4.1.5	Implementation . . . . .	26
4.2	Analysis of the model . . . . .	27
<b>5</b>	<b>The Wave equation method</b>	<b>30</b>
5.1	The model . . . . .	30
5.1.1	The wave equation . . . . .	30
5.1.2	Lumping the states . . . . .	32
5.1.3	Boundary conditions . . . . .	33

5.1.4	State-space model . . . . .	34
5.1.5	Implementation . . . . .	35
5.2	Analysis of the model . . . . .	35
5.2.1	Correction of energy absorption . . . . .	35
5.2.2	Results . . . . .	38
5.2.3	Domain of validity . . . . .	40
5.2.4	The purpose of the model . . . . .	41
<b>6</b>	<b>An extension of the model</b>	<b>44</b>
6.1	Implementation . . . . .	44
6.2	Results . . . . .	45
6.3	The purpose of the model . . . . .	45
<b>7</b>	<b>Conclusions and recommendations</b>	<b>47</b>
7.1	Recommended improvements . . . . .	47
	<b>References</b>	<b>50</b>
	<b>Appendix A: Mass spring method</b>	<b>51</b>
	<b>Appendix B: Wave equation method</b>	<b>54</b>
	<b>Appendix C: Evaluation of the models in MATLAB</b>	<b>57</b>

## List of Figures

2.1	The Common Rail Diesel Injection System. . . . .	3
3.1	A general picture of the model with input and output signals. . . . .	7
3.2	The high pressure pump. . . . .	8
3.3	The pump signal. . . . .	8
3.4	The duty cycle $c$ of the signal, where $c = (\frac{pulsewidth}{period})$ . . . . .	9
3.5	The pressure control valve. . . . .	9
3.6	An injector. . . . .	10
3.7	The water hammer phenomenon. . . . .	11
3.8	Oscillations near the valve caused by the water hammer phenomenon. . . . .	11
3.9	Measured pressure near an injector during injection. . . . .	12
3.10	DFT of the pumpsignal. . . . .	13
3.11	Lower frequencies in the pump signal spectrum. . . . .	14
3.12	DFT of the rail signal. . . . .	15

3.13	Lower frequencies in the rail signal spectrum. . . . .	16
3.14	DFT of the rail signal for different pressure levels. . . . .	17
3.15	DFT of the rail signal for different engine speeds. . . . .	18
4.1	A mechanical example. . . . .	19
4.2	A mechanical system that may serve as an approximation for the CR System. . . . .	20
4.3	A bonding. . . . .	21
4.4	Bondings showing intensity and flow storage. . . . .	22
4.5	A carriage attached to the wall by a spring and a dashpot. . . . .	22
4.6	A bondgraph showing the energy flow in the system described in figure. 4.5 . . . . .	23
4.7	The approximation of the CR System with all inputs added. . . . .	25
4.8	A bondgraph that describes the energy flow in the approxi- mated CR System. . . . .	26
4.9	The modelled signal and the validation signal. . . . .	28
4.10	Frequency spectra of the modelled signal and the validation signal. . . . .	29
5.1	Reflection of an acoustic wave at a closed end of a tube. . . . .	33
5.2	The model with inputs and outputs. . . . .	35
5.3	The validation signal and the modelled signals from positions at the end of the rail (p1) and in the middle (p10). . . . .	36
5.4	The frequency spectra of the rail signal and modelled signals from positions at the end of the rail (p1) and in the middle (p10). . . . .	37
5.5	The validation signal and the modelled signals from positions at the end (p1) and in the middle (p10) of the rail after correction of the damping factor. . . . .	38
5.6	The frequency spectra of the rail signal and modelled signals from positions at the end (p1) and in the middle (p10) of the rail after correction of the damping factor. . . . .	39
5.7	The modelled signal with the validation signal. . . . .	40
5.8	Frequency spectra of the validation signal and the modelled signal. . . . .	40
5.9	The modelled signals (solid lines) with the validation signals (dotted lines). . . . .	42
5.10	Measured signals at injector 1,2,5 and 6. . . . .	43
5.11	Modelled signals: p2, p5, p14 and p17. . . . .	43
6.1	The modelled signal (solid lines) with the validation signal (dotted lines). . . . .	46

---

A.1	The model implemented in SIMULINK. . . . .	51
A.2	The m-file where the physical parameters and the state space model are defined. . . . .	53
B.1	The model implemented in SIMULINK. . . . .	54
B.2	The m-file where the physical parameters and the state space model are defined. . . . .	56
C.1	The most important MATLAB code used to examine signals. . . . .	57

**List of Tables**

5.1	Working points . . . . .	41
6.1	Working points . . . . .	45



# 1 Introduction

## 1.1 Background

The Common Rail Diesel Injection System (CR System) is a relative new injection system for passenger cars. The main advantage of this injection system compared to others is that due to the high pressure in the system and the electromagnetically controlled injectors it is possible to inject the correct amounts of fuel at exactly the right moment. This implies lower fuel consumption and less emissions.

However at certain working conditions (i.e. different combinations of engine speed and pressure) the OM613 Common Rail Diesel Injection (CDI) Engine does not run smoothly. The reason may be that there is a significant difference in the injected fuel quantities among the injectors. Measurements show that the pressure at the injectors differ in behaviour, which may explain the varying injected amounts. The system can be described by superposition of many different pressure waves and a wave phenomenon may be present. If it is known how the total pressure wave along the common rail (which from now on will be named rail only) behaves, it may be possible to avoid the varying injected amount by either controlling the injectors separately or by moving the injector pipes to more favourable locations.

## 1.2 The thesis

This thesis is a study of the pressure waves generated in the Common Rail Diesel Injection System. The main aim of the thesis is to explain the behaviour of the pressure waves in the high pressure accumulator (rail) by developing a physical model of the real system in SIMULINK[1]. The purpose of the model is to get more information about what the total pressure wave in the rail looks like and to find out if wave phenomena, as for instance standing waves, are present in the rail. A further developed model may be used to supervise the function of the injections. To make sure that the model is possible to implement in a car, it is kept as simple as possible.

The system is very complex and therefore some approximations are necessary and the study is also limited to include normal operation behaviour of the system and static working conditions only.

## 1.3 Methods

Since the model is a physical model of the real system, all the equations are based on well known physical laws as the wave equation, Newton's laws etc.

The system is divided into subsystems in order to explain the behaviour of the whole system as accurately as possible.

Two different approaches are used. In the first method the system is approximated with a mass spring system which is modelled by using bond-graphs to structure the problem. The other approach is more strict and it generates a model from the continuous partial differential equation that describes the propagation of waves, the general wave equation. As a simplification the model is lumped by making the partial differential equation discrete. Boundary conditions that describe the physical behaviour at the ends of the rail, are determined and finally input signals are added to the system. Both models are implemented in SIMULINK.

## 1.4 Thesis Outline

The report is structured in the following way:

**Chapter 2, The Common Rail Diesel Injection System** A description of the CR System is given and its function is explained.

**Chapter 3, The Common Rail Diesel Injection System from a modelling point of view**  
The CR System is described from a modelling point of view. The input signals to the system and the validation signal are discussed and analysed.

**Chapter 4, The mass spring method** The mass spring modelling method is explained and the results are discussed.

**Chapter 5, The wave equation method** The modelling method based on the general wave equation is described and the results are analysed.

**Chapter 6, An extension of the model** A suggestion about how the model can be used at other working points than the one it was developed for, is presented.

**Chapter 7, Conclusions** Conclusions are drawn and recommendations are given.



## 2 The Common Rail Diesel Injection System

The CR System (figure 2.1) is an accumulator injection system used in passenger cars of Mercedes-Benz. It provides more flexibility than any previously used injection system, but it also needs to handle much higher pressure. A brief introduction to this system follows, but further information about this system can be found in [2].

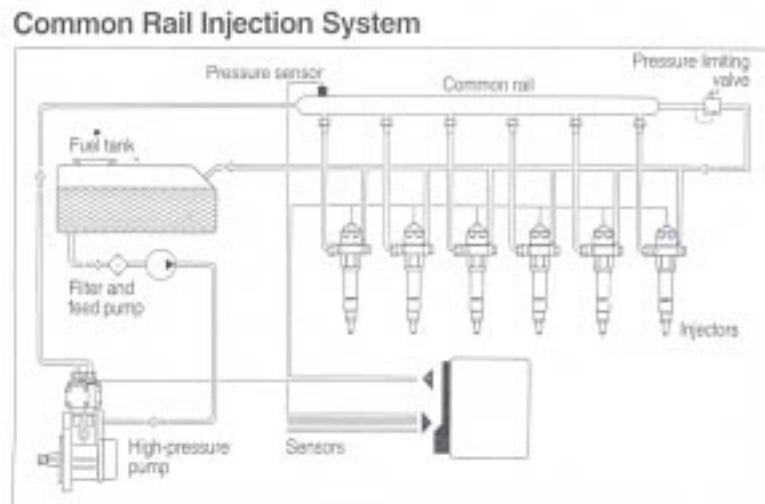


Figure 2.1: The Common Rail Diesel Injection System.

### 2.1 Injection systems

The CR System is an injection system used in direct-injection engines. It is common to differentiate between direct-injection (DI) engines and indirect-injection (IDI) engines. In IDI engines the fuel is injected into a prechamber in which the combustion is initiated [2]. In the DI engines the fuel is injected directly into the cylinder's combustion chamber. DI engines feature fuel savings of up to 20 percent compared with IDI engines, but the latter

generates less noise than the former. The advantage of the CR System is the high pressure in the rail, which makes it possible to use precise and highly flexible injection processes. Other injection systems are the VP44 radial-piston distributor pump and the PE in-line injection pump. The first system is an electronic diesel control (EDC) injection system in which the injections are controlled by a solenoid valve. Both the duration of the injection and the injected amount of fuel depend upon the time the valve is open and the system is accordingly named time-controlled injection system. In this system fuel supply, high pressure generation and fuel distribution are all combined in one component. The PE inline injection pump creates high pressure for each cylinder in its own high-pressure chamber. The system is called a helix-controlled injection system, since the duration of injections and the injected fuel quantity are functions of the position of the so-called helix with reference to a spill port. This system is suitable for providing large injected fuel amounts, which makes it commonly used in heavy truck engines.

The CR System system can be divided into three different functional groups

- The high pressure circuit
- The low pressure circuit
- The ECU (Engine Control Unit) with sensors

## 2.2 The high pressure circuit

The high pressure circuit contains a high-pressure pump, a pressure-control valve, a high pressure accumulator (the rail) with a rail-pressure sensor, high pressure connection lines and the injectors (see figure 2.1). This part of the CR System is responsible for generating a stable high pressure level in the rail and for injecting the fuel into the engine's combustion chambers. The high-pressure pump forces the fuel into the rail and generates a maximum pressure of 1350 bar. There is one injector for each cylinder and the injectors contain a solenoid valve which receives a current signal as an 'open' command from the ECU at the time for injection. Every time an injection occurs, fuel is taken from the rail. The pressure control valve attempts to keep the pressure at the desired level. This control is based on measurements from the rail pressure sensor.

**2.3 The low pressure circuit**

The low pressure circuit provides the high pressure part with fuel. The fuel is drawn out of the tank by a pre-supply pump and forced through the lines and through a fuel filter to the high-pressure pump in the high pressure circuit. Uninjected fuel from the rail is led back to the tank through the pressure control valve.

**2.4 The ECU with sensors**

The ECU evaluates signals from different sensors and supervises the correct functioning of the injection system as a whole. The main tasks for the ECU in the CR System are to keep the pressure in the rail at a desired level by controlling the pressure control valve, and to start and terminate the actual injection processes. Some of the quantities that the ECU calculates from the sensor measurements (e.g. rail pressure, engine speed, accelerator-pedal position and air temperature) are the correct quantities for fuel injections and the optimal start and duration of the injections.

### 3 The Common Rail Diesel Injection System from a modelling point of view

The CR System has already been modelled by using neural networks [3]. For this method a huge number of data-sets is needed to get reliable results. The idea of modelling the system physically was brought up in order to develop a method to estimate the injected fuel quantities as well as to find out more about the wave phenomena in the rail.

In this chapter, the physical behaviour of the different parts of the system will be described. The desired properties of the model are also stated here.

#### 3.1 The aim of the model and the desired properties

The main aim of the model is to explain the behaviour of the pressure waves in the high pressure accumulator of the system. The desired information is pressure signals from points along the rail. By comparing these signals it may be possible to understand why the measured pressure signals at the injectors differ. If a standing wave phenomenon is present, it would be shown in the model as well.

Since points along the rail are most interesting, the waves in the system are approximated to only propagate in one dimension. The model is developed for the working point with an engine speed of 2300 rpm, a pressure level in the rail of 800 bar and a temperature of 40.5°, and then an analysis is made to examine the domain of validity. The flow of the fuel in the rail is neglected in comparison with the speed of a pressure wave in the fuel. This can be done since the speed of the pressure wave is so high (i.e. between 1350-1480 m/s depending on the working conditions).

#### 3.2 Measured signals used in the model

A general description of the model with input and output signals is given in figure 3.1. The pump signal is a pressure signal measured at the end of the rail where the pipe from the pump is connected, when the system is running normally except that there are no injections. This signal is used as an input to the system at this point. The injection signals are measured at the valve ends of the injection pipes. The signal from one injector pipe (the sixth) is used as input at all the 6 points where the injection pipes are connected to the main rail. The reason for this is that, apart from a time delay, these signals are supposed to be equal. The result of the difference in the signals is not of interest in this study. The aim is to find out what happens in the

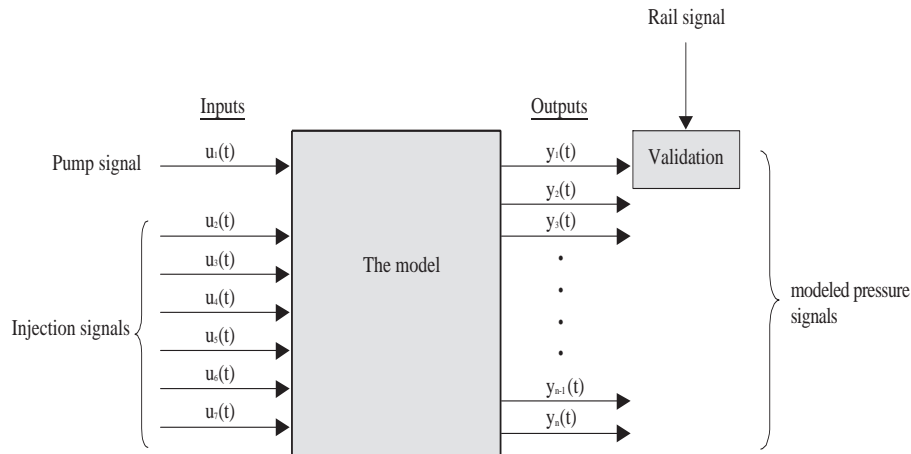


Figure 3.1: A general picture of the model with input and output signals.

rail when everything works properly. The rail signal is measured by the same sensor as the pump signal but with injections. This signal is the only available validation signal. The pressure at points along the rail are outputs from the model. It is interesting to compare these outputs with the injection signals to see that the general shape of the signals are the same. Frequencies above 2000 Hz are considered as noise and all the measured data sets are lowpass filtered with this cut-off frequency before they are used.

### 3.2.1 The pump

The high pressure pump, shown in figure 3.2, is connected to the camshaft and therefore driven with half the engine speed. It contains three pump plungers which are pumping fuel into the high pressure pipe that leads to the main rail. In an ideal situation the pressure signal from the pump would have been a constant signal. In reality the signal contains mainly three sinus-waves with different phase. The main frequency of this signal is therefore three times the frequency of the pump (i.e. the frequency of half the engine speed), which means around 57 Hz at an engine speed of 2300 rpm <sup>1</sup>. The sinus waves derive from the motions of the pump plungers in the pump. The pump signal is shown in figure 3.3.

<sup>1</sup> $(\frac{3 \cdot N}{2 \cdot 60})Hz = (\frac{3 \cdot 2300}{2 \cdot 60})Hz = 57.5Hz$ , where  $N$  is engine speed.

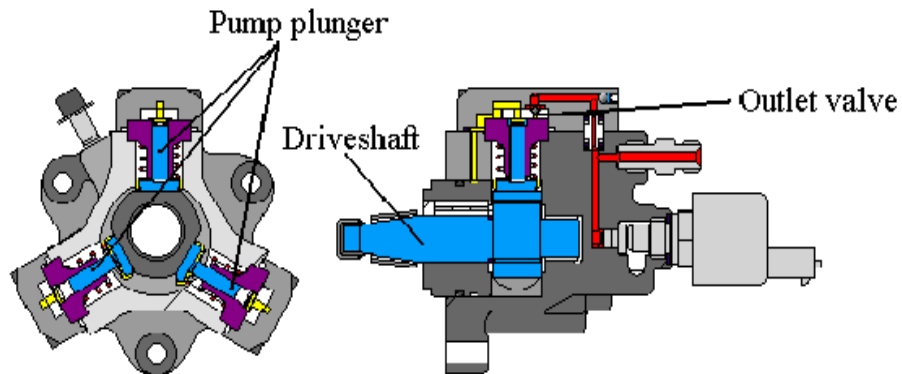


Figure 3.2: The high pressure pump.

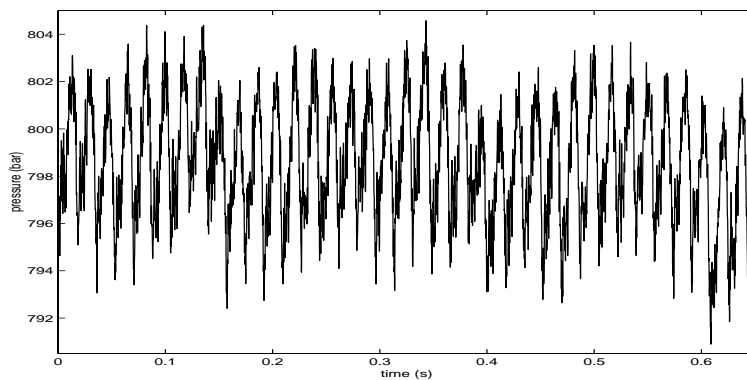


Figure 3.3: The pump signal.

### 3.2.2 The pressure control valve

The pressure control valve at the end of the rail is electromagnetic and it is controlled by a rectangular pulse signal from the ECU. The frequency of the signal is always around 1000 Hz, but the duty cycle, the relative width of the pulses (see figure 3.4), depends on the mean pressure at each working point. The ECU gets information about the pressure level from the sensor in the rail and calculates an adequate pulse width. The current pulse from the ECU controls a ball that is located in the middle of the opening as figure 3.5

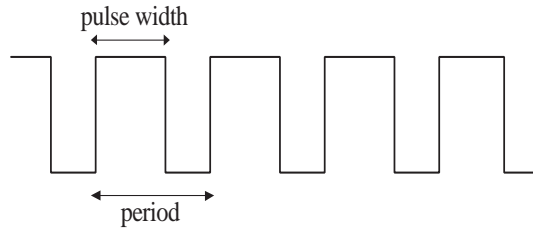


Figure 3.4: The duty cycle  $c$  of the signal, where  $c = (\frac{pulsethickness}{period})$ .

shows. For a certain pressure level the ball is expected to stand still since the frequency of the pulses is quite high. Nevertheless a 1000 Hz frequency component is found when frequency analyses of the pump signal and the rail signal are made. It can be assumed that this derives from the current pulse. The reader is referred to subsection 3.6 for a further discussion about the frequencies.

### 3.2.3 The injectors

The injectors are responsible for injecting fuel into the combustion chamber. The amount of injected fuel and the time for injections are determined by the ECU and control signals are sent to the electromagnet in the injector

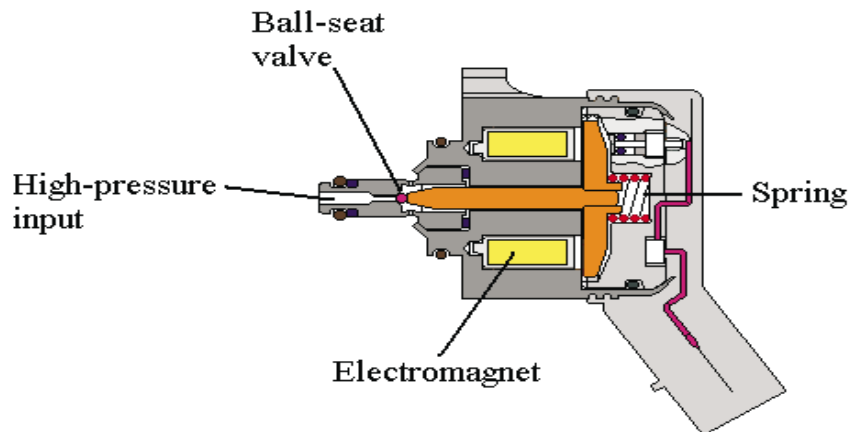


Figure 3.5: The pressure control valve.

(see figure 3.6). The opening and closing of the valve in the injector are then controlled by the electromagnet. First there is a pilot injection and

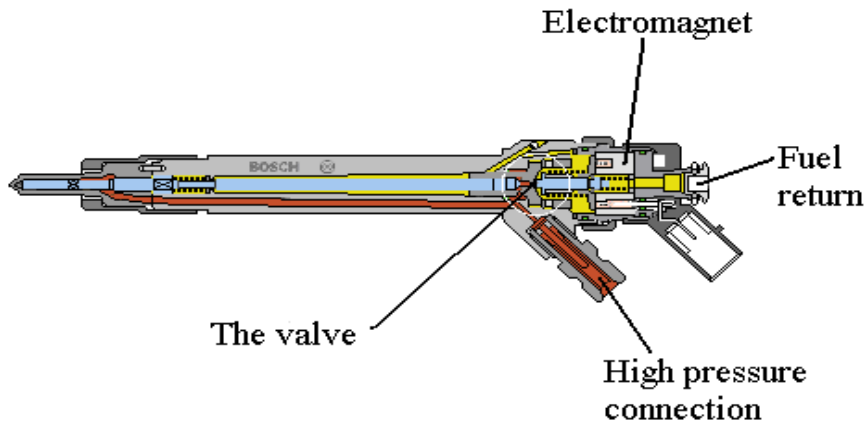


Figure 3.6: An injector.

then a main injection. Since the valve in the injector is closed very quickly, a so-called water hammer is formed in the injector pipe. This phenomenon will be described briefly here, for a more detailed explanation the reader is referred to [4].

The water hammer is created when a valve is closed quickly in a pipe. To be able to describe the phenomenon the flow of the fluid can not be neglected. Consider the valve in the injector to be open and a flow in the injector pipe. There is an initial pressure  $p_0$  and an initial velocity  $v$  in the pipe as shown in (figure 3.7a). Suddenly the valve is closed, which creates a pressure wave that travels toward the main rail. The fluid between the wave and the valve will be at rest but the fluid between the wave and the rail will still have the initial velocity  $v$  (figure 3.7b). When the wave reaches the main rail the whole pipe will have the pressure  $p_0 + \Delta p$ , but the pressure in the rail will still be  $p_0$ . This imbalance of pressure makes the fuel flow from the pipe back to the rail with the velocity  $v$  and a new pressure wave is created and it travels toward the valve end of the pipe (figure 3.7c). When the wave reaches the end, the fluid is still flowing. The pressure at this point will be less than the initial value,  $p_0 - \Delta p$ . This leads to a rarefied wave of pressure in the other direction (figure 3.7d). When this wave reaches



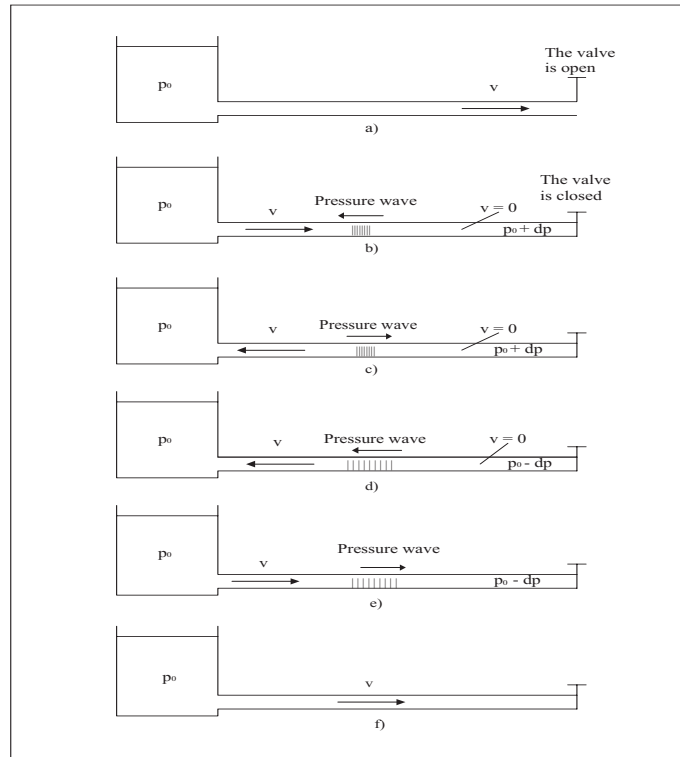


Figure 3.7: The water hammer phenomenon.

the rail, the pipe will have a pressure less than that in the rail. There is an imbalance in pressure again and the process repeats itself in a periodic manner (figures 3.7e and 3.7f). The result is an oscillation which is damped

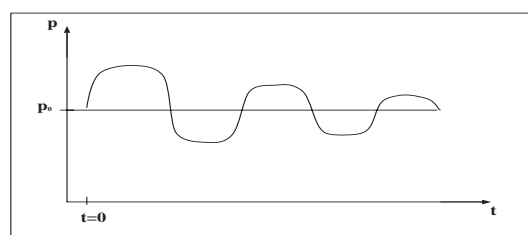


Figure 3.8: Oscillations near the valve caused by the water hammer phenomenon.

because of viscous effects as figure 3.8 shows. First when an injection occurs the valve opens and there is a pressure drop as result. Then the valve is

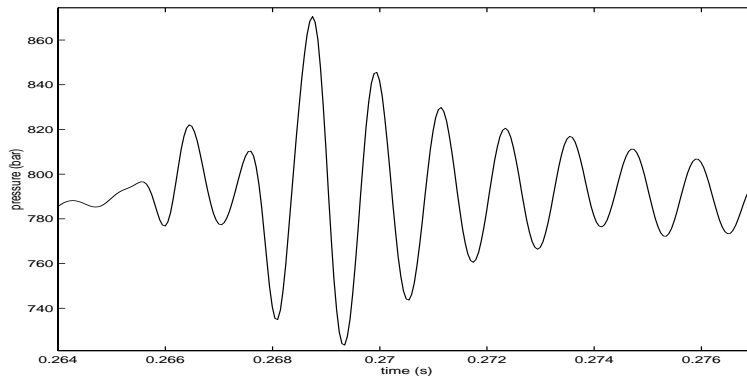


Figure 3.9: Measured pressure near an injector during injection.

closed quickly and the water hammer phenomenon appears. Because of the pilot and the main injection the pressure signal gets an appearance of two damped oscillations after each other as shown in figure 3.9.

A model of the injection pipe is developed in a similar manner as the model of the main rail. As an input to this model one of the injection signals is used (see section 3.2). The output from this model is damped and a bit time delayed, but apart from this, the signal is similar to the input. In order to reduce the number of states of the whole model, this submodel is replaced by a damping constant only. The signal is also delayed with the corresponding time it takes for the pressure wave to travel through the injector pipe. The time derivative of this signal is then used as injector inputs to the model. The signals are triggered to agree with the actual opening of the injectors.

### 3.3 Frequency analysis

To understand the system better the frequencies of the measured signals are analysed. The first signal to be discussed is the pump signal, i.e. the rail pressure measured without injections. Then the rail signal is analysed, the measured signal from the same sensor but with injections. The first signal is used as an input to the model and the latter one is used to validate the model. The signals that are analysed are recorded at the working point for the model (i.e. 2300 rpm, 800 bar, 40.5°C).

**3.3.1 The pump signal**

In figure 3.10 a DFT of the pump signal is shown. The DFT is generated in MATLAB [5] by first subtracting the mean value from the signal, using zeropadding in order to get better frequency resolution and then using the fft algorithm. In figure 3.11 the lower frequencies are zoomed in. The

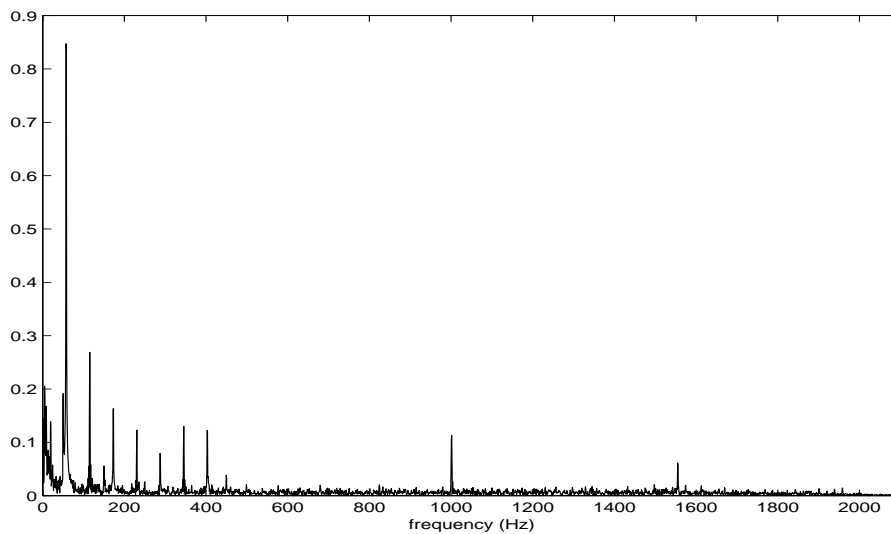


Figure 3.10: DFT of the pumpsignal.

frequency with highest amplitude is the one around 57 Hz. This is the main frequency component in the signal from the pump. As explained earlier in this chapter, the pump is driven with half the engine speed. At this working point the engine speed is 2300 revolutions per minute, which implies a frequency of 38.33 Hz. Since there are three pump plungers in the pump, the main frequency in the generated pressure signal will be  $\frac{3 \cdot 38.33 \text{ Hz}}{2} = 57.5$  Hz. The first multiple of this frequency is  $2 \cdot 57.5 \text{ Hz} = 115$  Hz which is also found in figure 3.11. In the same manner the five following multiples can be calculated and found in the spectrum at 172.5, 230, 287.5, 345 and 402.5 Hz. At 1000 Hz a frequency is found which most likely comes from the pressure control valve, since it is controlled by a current pulse with this frequency. If frequency spectra of the rail signal for many different working points (see figure 3.14 and figure 3.15) are studied, the 1000 Hz peak is visible for almost all workings points. This also indicates that this frequency comes from the pressure control valve. There is also a high amplitude at the frequency 50 Hz. This component is traced to the injectors by analysing the frequencies

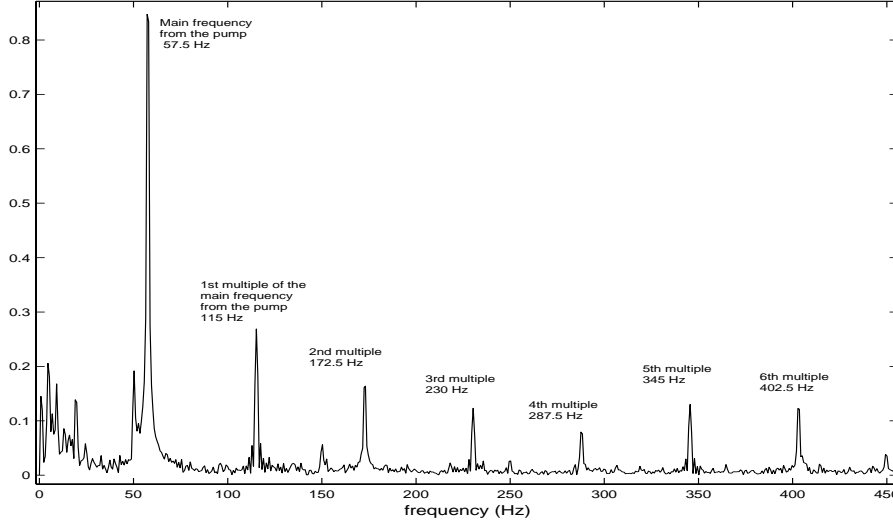


Figure 3.11: Lower frequencies in the pump signal spectrum.

from signals measured at the injectors both with and without injections. The peak at 50 Hz is a main component in these frequency spectra and the amplitude of this frequency component is much higher here than in the spectrum of the pump signal. Since this frequency component has the same amplitude in both spectra from the injector signals (with and without injections), it can be assumed to derive from a constant influence from the injectors. There is also a peak at 1555 Hz, but it is not obvious where it derives from. If a standing wave phenomenon is present in the rail the frequencies of this wave would depend on the length of the rail and the speed of the wave  $v$  (at this working point) in the following way

$$f_{ri} = \frac{k \cdot v}{\lambda_{ri}} \quad (3.1)$$

where  $f_{ri}$  means the frequencies of possible standing waves in the rail and  $k$  is the harmonic number which identifies the order of the standing wave [6]. The first possible standing wave, which implies  $k = 1$ , has a wavelength  $\lambda_{r1}$  which is double the length  $l_r$  of the rail, since this is the simplest case when a standing wave can occur. This means that the lowest frequency for a standing wave at the analysed working point becomes

$$f_{r1} = \frac{1 \cdot 1400}{\lambda_{r1}} = \frac{1400}{2 \cdot 0.524} = 1335.87 Hz \approx 1336 Hz \quad (3.2)$$

The lowest possible frequencies for possible standing waves in the injection pipes  $f_{i1}$  and in the pump pipe  $f_{p1}$  are

$$f_{p1} = \frac{1400}{2 \cdot 0.505} = 1386.13Hz \approx 1386Hz \quad (3.3)$$

and

$$f_{i1} = \frac{1400}{2 \cdot 0.154} = 4545.45Hz \approx 4545Hz \quad (3.4)$$

Even if the 1555 Hz peak differs a lot from the lowest standing wave frequency, it can not be excluded that it is caused by this wave phenomenon. But when the spectrum of the pump signal is compared with a spectrum of the same sensor signal but with injections, the amplitude of this frequency increases a lot in the latter case (see figure 3.12). If it was caused by a standing wave the amplitude would remain on almost the same level. Another possibility is that the 1555 Hz frequency comes from the pump and the injections since 1610 Hz is a multiple of both 57.5 Hz and 115 Hz <sup>2</sup>. But as shown in figure 3.14 this peak varies in frequency along the pressure axis. If this frequency component derives from the main frequencies of the pump and the injections, the peak would only move on the frequency axis when the engine speed is varied. It is also difficult to determine where the

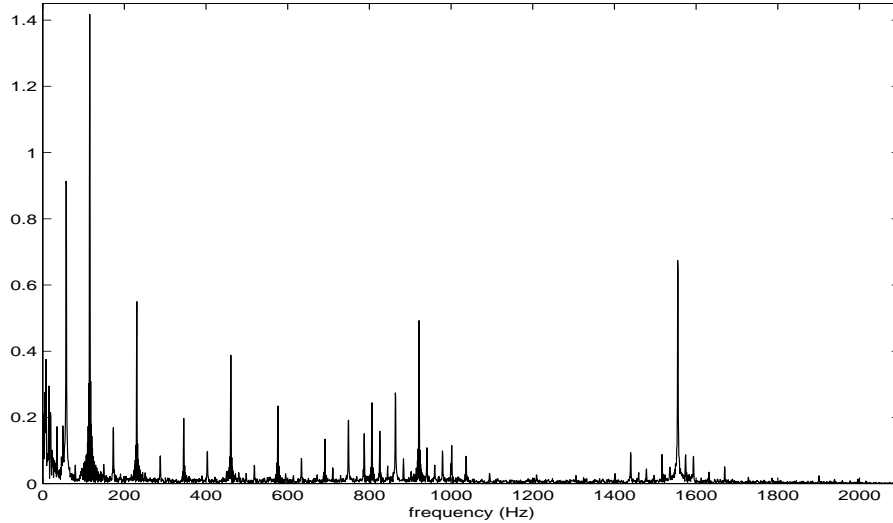


Figure 3.12: DFT of the rail signal.

frequencies below 40 Hz come from. It may be slow changes in the valve or

<sup>2</sup> $14 \cdot 115Hz = 1610Hz$  and  $28 \cdot 57.5Hz = 1610Hz$

in the injectors which get more powerful with injections than without, since the amplitudes of the frequencies are higher in the DFT of the signal with injections.

### 3.3.2 The rail signal

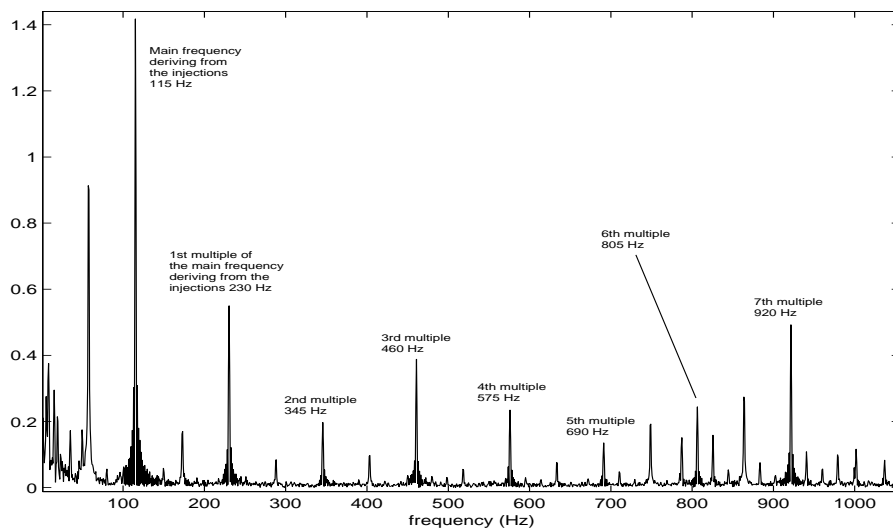


Figure 3.13: Lower frequencies in the rail signal spectrum.

A DFT of the rail signal is produced in the same way as the DFT of the pump signal and it is shown in figure 3.12. Besides the frequencies from the pump described above, there is a series of multiple frequencies coming from the injections. For this working point (engine speed 2300 rpm) there are 6 injections each cycle (0.052 s), which leads to a main frequency at 115 Hz for the injections. Since this is also a multiple of the main frequency from the pump, the amplitude of this frequency becomes high. In figure 3.13, the multiples of the main frequency from the injections are marked. The damped oscillations in the injection signals result in many frequencies between 700 and 1000 Hz. There are different frequencies in all the injection signals and the signals affect each other, which makes it difficult to determine the source of a certain frequency.

**3.3.3 Other working points**

In figures 3.14 and 3.15 frequency spectra for different working points are shown. Both spectra are developed from data sets with injections. In figure 3.14 the engine speed is fixed at around 2300 rpm and the pressure level is varied. As the mean pressure increases the amplitudes of the frequencies belonging to the pump and the injections increase as well. The reason is that the amplitude of the pump signal (in the time domain) rises with the pressure. The frequencies around 800-900 Hz, from the damped oscillations in the injection signals, show a pattern of interest. The amplitude of this frequency region is varying a lot along the pressure axis. It is natural that the working points with lower pressure also get lower frequency amplitudes, but the behaviour around 900 bar is difficult to explain. In this spectrum (figure 3.14) a movement along the frequency axis for the frequencies around 1500 Hz is visible. It seems to be a peak that increases in frequency with increasing pressure. This phenomena does not appear in figure 3.15, which derives from data sets measured with mean pressure around 800 bar and with varied engine speed. This means that the cause of this frequency depends on pressure but not on the engine speed. The increase in amplitude

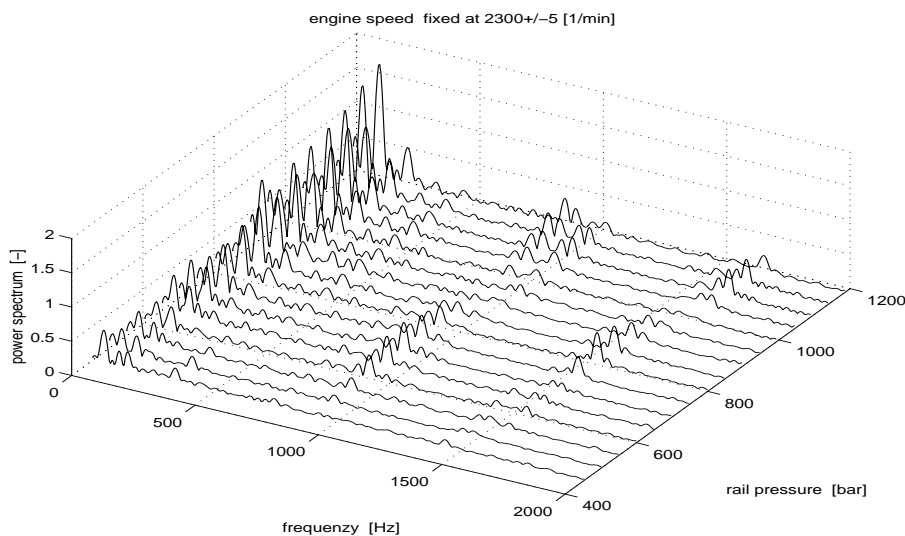


Figure 3.14: DFT of the rail signal for different pressure levels.

of the frequencies from the pump and the injections (50-150 Hz) at lower engine speed depends most likely on a compensation in pressure by the pump for the slower running engine (see figure 3.15).

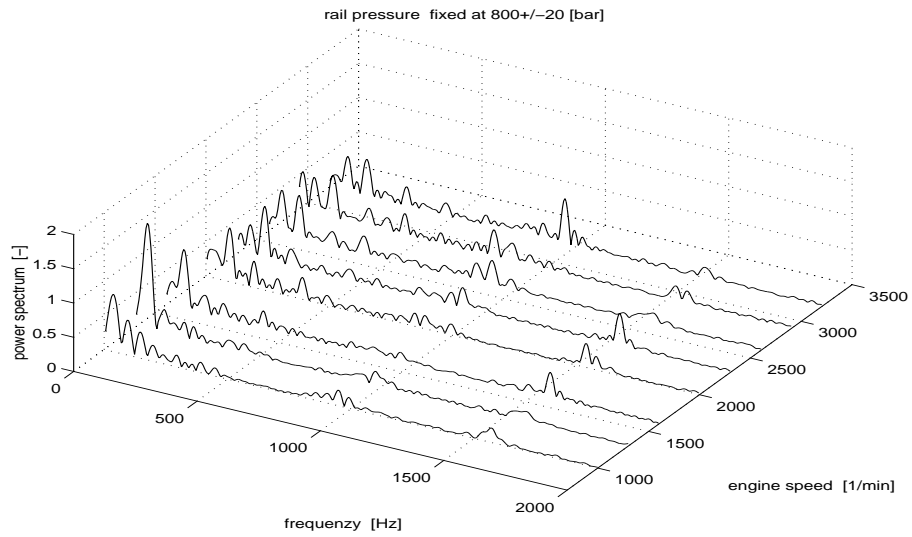


Figure 3.15: DFT of the rail signal for different engine speeds.



## 4 The Mass spring method

This modelling method is based on the fact that the pressure wave can be approximated by a mechanical wave travelling in a system of masses with springs and damping dashpots in between them.

### 4.1 The model

The model is developed by using established equations such as Newton's motion law's and Hooke's law to described the mechanical system. Bondgraphs are used to transfer the equations to state space form before implementing them in SIMULINK.

#### 4.1.1 The basic equation

Consider a carriage with a mass  $m$  moving frictionless on a plane as shown in figure 4.1a. This carriage is attached to the wall via a spring with spring

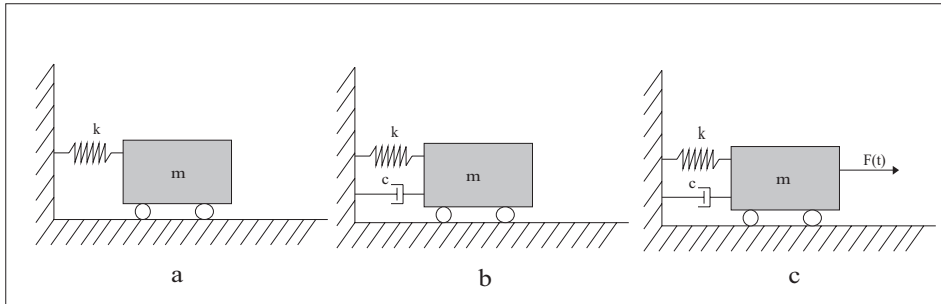


Figure 4.1: A mechanical example.

constant  $k$ . The motion of this mass  $m$  can be described as follows [7]:

$$\ddot{\xi}(t) \cdot m = -k \cdot \xi(t) \quad (4.1)$$

where  $\xi(t)$  is the displacement from the equilibrium position. If a damper with a damping factor  $c$  is added to the system as shown in figure 4.1b, this will affect the system in a resistive way:

$$\ddot{\xi}(t) \cdot m = -k \cdot \xi(t) - c \cdot \dot{\xi}(t) \quad (4.2)$$

If the mass element is driven by an external force  $F(t)$  the equation of motion of the mass element is given by

$$\ddot{\xi}(t) \cdot m + k \cdot \xi(t) + c \cdot \dot{\xi}(t) = F(t) \quad (4.3)$$

and such a system is shown figure 4.1c. The fluid in the CR System can be described by many masses with springs and damping dashpots in between them. The mechanical wave caused by the force  $F(t)$  corresponds to the pressure wave propagating in the medium. The whole rail can be modelled as shown in figure 4.2.



Figure 4.2: A mechanical system that may serve as an approximation for the CR System.

#### 4.1.2 Bondgraphs

To make the modelling of a system more systematic, bondgraphs can be used to follow the energy flow in the system. By studying the energy exchange and knowing that energy is undestroyable, this method guarantees that nothing is forgotten. An introduction to bondgraphs is given here, for further information the reader is referred to [8].

The essential idea of bondgraphs is that many models can be described in terms of intensity variables  $e$  (effort) and flow variables  $f$  (flow). In an electrical system for instance, the intensity is voltage  $u(t)$  and the flow is current  $i(t)$ . Simple electrical systems that contain resistors, coils and capacitors can be described by using the following common relations

$$u(t) = L \cdot \frac{d}{dt}i(t) \iff i(t) = \frac{1}{L} \int_0^t u(s)ds \quad (4.4)$$

$$i(t) = C \cdot \frac{d}{dt}u(t) \iff u(t) = \frac{1}{C} \int_0^t i(s)ds \quad (4.5)$$

$$u(t) = R \cdot i(t) \quad (4.6)$$

where  $L$  is the inductance,  $C$  is the capacitance and  $R$  is the resistance. In a resistor electrical energy is transferred to heat energy. In a coil and in a capacitor energy is stored as magnetic and electrical field energy respectively.

In an equivalent way intensity and flow are found as force  $F(t)$  and velocity  $v(t)$  in a mechanical system. A mechanical system without any rotations can be described by Newton's law and Hooke's law of elasticity:

$$F(t) = m \cdot \frac{d}{dt}v(t) \iff v(t) = \frac{1}{m} \int_0^t F(s)ds \quad (4.7)$$

$$\begin{aligned} F(t) &= k \cdot \xi(t) \\ \frac{d}{dt}\xi(t) &= v(t) \end{aligned} \iff F(t) = k \cdot \int_0^t v(s)ds \quad (4.8)$$

$$F(t) = c \cdot v(t) \quad (4.9)$$

where  $k$  is the spring constant,  $m$  is the mass of the object and  $c$  is the damping constant of a dashpot. The velocity of the object and the compressed spring correspond to storage of kinetic and elastic energy. In the damping dashpot energy transfers to heat energy as in the resistance in the electrical case described above.

The bondgraph as a whole shows the energy flow in a system and the bonding itself connects subsystems which are exchanging energy. The half arrow indicates in which direction energy flows if the product  $e \cdot f$  is positive (see figure 4.3). As explained earlier many physical elements result in a

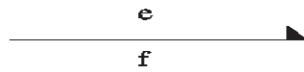


Figure 4.3: A bonding.

storage of energy. The storage can either be capacitive or inductive. The capacitive storage is found in the capacitor in the electrical case and in the compressed spring in the mechanical case. The inductive storage on the other hand is found in the coil in the first case and in the object's velocity in the latter case. This is marked in the bondgraph in figure 4.4. The bonding symbolizes that energy flows from the rest of the system, which is assumed to be on the left hand side of the bonding, into the element on the right hand side. If the relation between  $e$  and  $f$  is linear

$$e(t) = \frac{1}{b} \int^t f(\tau)d\tau \quad (4.10)$$

or

$$f(t) = \frac{1}{a} \int^t e(\tau)d\tau \quad (4.11)$$

the proportional constant is marked in the system as shown in figure 4.4. For resistive elements such as a resistance in the electric system or a dashpot

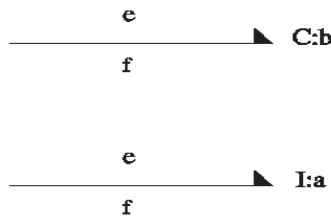


Figure 4.4: Bondings showing intensity and flow storage.

in the mechanical system, following relation is valid:

$$e(t) = f(t) \cdot c \quad (4.12)$$

In this case the bondgraph is marked  $R : c$ . Inputs to a system are called sources and are marked  $S_e$  or  $S_f$  depending on whether the input signal is intensity or flow. To connect different bondings, junctions are needed. The two most important junctions are parallel and series junctions. In a parallel junction all the bondings have to have the same flow,  $f_1 = f_2 = \dots = f_n$ , and the sum of all the intensities has to be zero,  $e_1 + e_2 + \dots + e_n = 0$  (an arrow directed out from a junction means change of sign). In a series junction, the conditions are reverse, the sum of the flows has to be zero and all the intensities have to have the same value.

A short mechanical example will illustrate the bondgraph method. Consider the system introduced in the beginning of this chapter (figure 4.5). A carriage with mass  $m$ , which moves frictionless on the ground, is attached to the wall by a spring with spring constant  $k$  and a dashpot with a damping constant  $c$ . A force  $F(t)$  is applied to the carriage which gets a velocity  $v(t)$ . The force is then considered as an input to the system which results in an

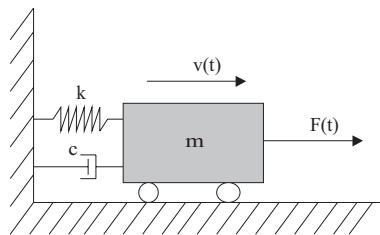


Figure 4.5: A carriage attached to the wall by a spring and a dashpot.

intensity source in the bonding graph. The energy applied to the system will be divided into the carriage's kinetic energy, energy loss in the dashpot

and energy storage in the spring. The kinetic energy corresponds to intensity storage and in the spring flow is stored. The carriage as well as the spring and the dashpot will be influenced by a velocity  $v(t)$  and therefore there will be a series junction in the bondgraph (see figure 4.6). When the

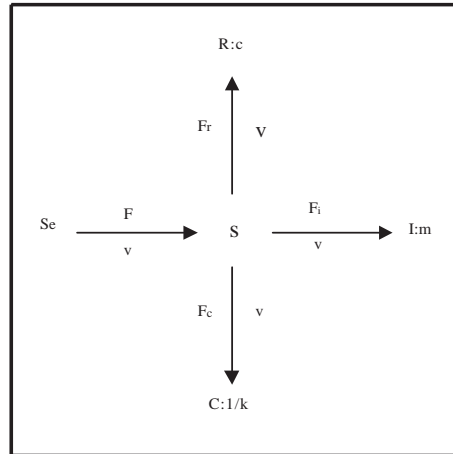


Figure 4.6: A bondgraph showing the energy flow in the system described in figure. 4.5

graph is completed it contains all the information needed to form a state space model. The following relations can be obtained from the bondgraph in figure 4.6:

$$\begin{aligned}
 S_e & : F(t) \\
 s & : F(t) - F_r(t) - F_i(t) - F_c(t) = 0 \\
 C : \frac{1}{k} & : F_c(t) = k \int_0^t v(\tau) \tau \\
 I : m & : v(t) = \frac{1}{m} \int_0^t F_i(\tau) d\tau \\
 R : c & : F_r(t) = c \cdot v(t)
 \end{aligned}$$

When bondgraphs are used, the choice of states becomes natural. The intensity and flow storage can be considered as the memory of the system, wherefore all the storing elements should be given one state each. The following state space system with  $x_1 = v(t)$ ,  $x_2 = F_c(t)$  and  $u(t) = F(t)$  is

a possible solution:

$$\begin{bmatrix} \dot{x}_1(t) \\ \dot{x}_2(t) \end{bmatrix} = \begin{bmatrix} -\frac{c}{m} & -\frac{1}{m} \\ k & 0 \end{bmatrix} \mathbf{x}(t) + \begin{bmatrix} 0 \\ \frac{1}{m} \end{bmatrix} \mathbf{u}(t)$$

### 4.1.3 The Bondgraph method applied to the CR System

The CR System can generally be explained as shown in figure 4.2. Furthermore the pressure signals coming from the injection need to be added. To transform these pressure signals to force signals the following relation is used

$$p(t) = \frac{F(t)}{A_{inj}} \quad (4.13)$$

where  $A_{inj}$  is the cross section area of the injector pipe. To get information about the pressure in the system the behaviour of the spring is used. The spring itself has similarities to a fluid where atoms can either be pressed together or drawn apart. In a spring the characteristic spring constant shows how easily this is done, in the fluid it is the compressibility constant. The two following relations show the similarity

$$F(t) = -k \cdot \xi(t) \quad (4.14)$$

$$p(t) = -K \cdot \Delta V(t)/V \quad (4.15)$$

where  $\Delta V/V$  is the relative change in the fluids volume,  $K$  is the compressibility constant and  $k$  is the spring constant. This means that the pressure at a certain point along the rail can be described by a function of the force acting upon the spring at this point. An extension or a compression of a spring corresponds to a deviation in pressure from an equilibrium level. The following relations are used

$$\xi(t) > 0 \quad \leftrightarrow \quad p(t) < p_0$$

$$\xi(t) = 0 \quad \leftrightarrow \quad p(t) = p_0$$

$$\xi(t) < 0 \quad \leftrightarrow \quad p(t) > p_0$$

where  $\xi(t)$  represents the extension ( $\xi(t) > 0$ ) or compression ( $\xi(t) < 0$ ) of the spring and  $p_0$  relates to the equilibrium pressure. The relations can be summarized by the following equation:

$$p(t) = p_0 - C \cdot \xi(t) \quad (4.16)$$

where  $C$  is a positive constant. The expression can be rewritten by using equation 4.14:

$$p(t) = p_0 + C \cdot \frac{F(t)}{k} \quad (4.17)$$

In this way the pressure can be derived from the states in the model. The constant  $C$  is determined by using the data sets without injections. The physical similarity between a spring and a fluid also implies that an input pressure signal along the rail can be added to the system, shown in figure 4.2, by adding forces that act upon the two nearest masses (an approximation that depends on the one-dimensional case). The system with all the inputs is shown in figure 4.7.

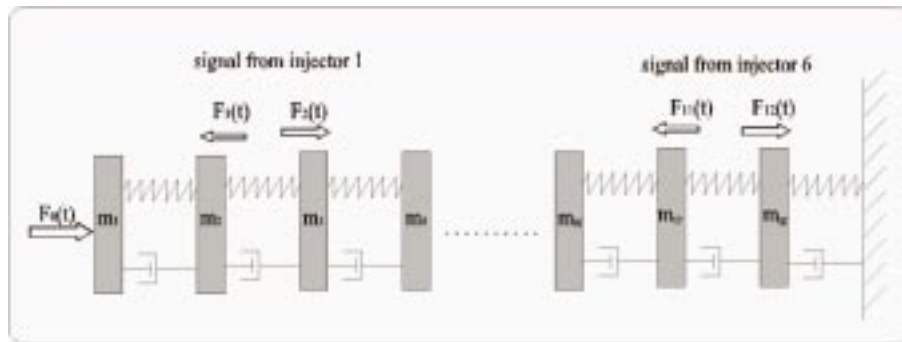


Figure 4.7: The approximation of the CR System with all inputs added.

The bondgraph from the example with the carriage, can be extended with extra subsystems to explain the CR System. The whole system is described by the general bondgraph in figure 4.8.

#### 4.1.4 Boundary conditions

The boundary conditions of the model are shown in figure 4.7. The wave is assumed to be completely reflected at the valve end of the rail and not reflected at all at the other end. The conditions would be more in accordance to reality if they could describe a partial reflection, but for this system such a description is not found. According to these circumstances it may also be more accurate to describe a total reflection at both ends. But the boundary conditions that are used now is a first approximation of the behaviour at the ends. If the mass spring method of modelling the system would have shown better results and better prospects of development (see section 4.2

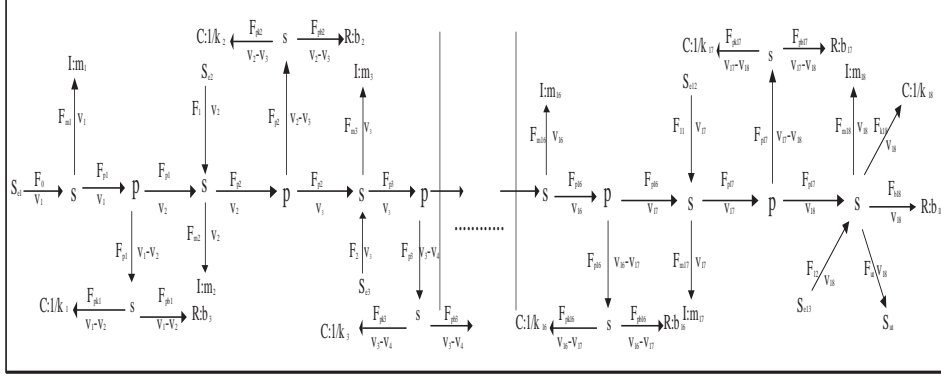


Figure 4.8: A bondgraph that describes the energy flow in the approximated CR System.

for an analysis of the model), this part of the model would be an object for further studies.

#### 4.1.5 Implementation

The physical parameters are estimated in the following way. All the masses  $m_i$ , the spring constants  $k_i$  and the damping constants  $c_i$  are assumed to be equal since the system is uniform. The volume of the rail  $V_{rail}$  and the density  $\rho$  at the working point are used to determine  $m_i$  in the following way:

$$m_i = \frac{V_{rail} \cdot \rho}{18} \quad (4.18)$$

The division by 18 is explained by the number of masses. The length  $l_i$  of an unaffected spring is estimated by dividing the total length of the rail into 18 equal parts. The volume of each part of the rail is  $V_i$ . When the spring constant is estimated, the spring's similarity to a fluid is used again. The compressibility constant  $K$  for the fluid is known and by using equations 4.13, 4.14 and 4.15 the following relation between  $K$  and  $k_i$  is found

$$\begin{aligned} K &= -\frac{p(t) \cdot V_i}{\Delta V_i(t)} = -\frac{F(t) \cdot V_i}{A_{rail} \cdot \Delta V_i(t)} = -\frac{F(t) \cdot \pi r_{rail}^2 l_i}{\pi r_{rail}^2 \cdot \pi r_{rail}^2 \cdot \xi(t)} = \\ &= -\frac{F(t) \cdot l_i}{\pi r_{rail}^2 \cdot \xi(t)} \approx \frac{k_i \cdot \xi(t) \cdot l_i}{\pi r_{rail}^2 \cdot \xi(t)} = \frac{k_i \cdot l_i}{\pi r_{rail}^2} \end{aligned}$$

where  $A_{rail}$  is the cross section area of the rail,  $V_i$  is the volume of one part ( $\frac{1}{18}$ ) of the rail,  $\Delta V_i(t)$  is the volume difference in this part when the fluid



is compressed compared to an equilibrium state and  $\xi(t)$  corresponds to the actual compression. The estimation is based on the assumption that the force acting upon a cross section area of the fluid in the rail can be regarded as the force acting upon a spring and this explains the approximate equal sign in the second last part of the expression. The spring constant can in other words be estimated by

$$k_i = \frac{K \cdot \Pi r_{rail}^2}{l_i} \quad (4.19)$$

The damping constant  $c_i$  is estimated by simulating the model and using data sets without injections.

As figures 4.7 and 4.8 show, the mechanical system contains repeating subsystems. These subsystems are described separately in different state space systems and put together in SIMULINK (see Appendix A).

## 4.2 Analysis of the model

To find out how well the model describes the system, it has to be validated. This means that the behaviour of the model is compared with the behaviour of the system and that the difference is evaluated. In this study this is done by comparing the rail signal with the corresponding modelled signal in both the time and the frequency domain.

Since the mass spring method approximates the CR System with a mechanical system, the approximation itself is a significant source of error. Physical parameters as the masses, the spring and the damping constants, have to be estimated by comparing the two systems, but none of them can be determined exactly. It is also difficult to estimate the initial values for the states since they are velocities and forces in an artificial system. It is natural to set all the initial conditions to zero then, but this leads to a long settling time for the output signals. However the model manages to describe some of the main features in the system, which is shown in figure 4.9. The model seems to produce a signal which corresponds to the mean values of the validation signal. There are neither really deep drops nor high peaks in the modelled signal, which indicates that the influence by the injection signals is slight. The signals may be too much damped. In figure 4.10 the frequency spectra of the validation signal and the modelled signal are shown. The most obvious difference is the accumulation of frequencies around 600-700 Hz in the spectra of the modelled signal. The cause of this cluster of frequency components is difficult to explain, but it seems to be related to the frequencies deriving from the damped oscillations in the injection signals,

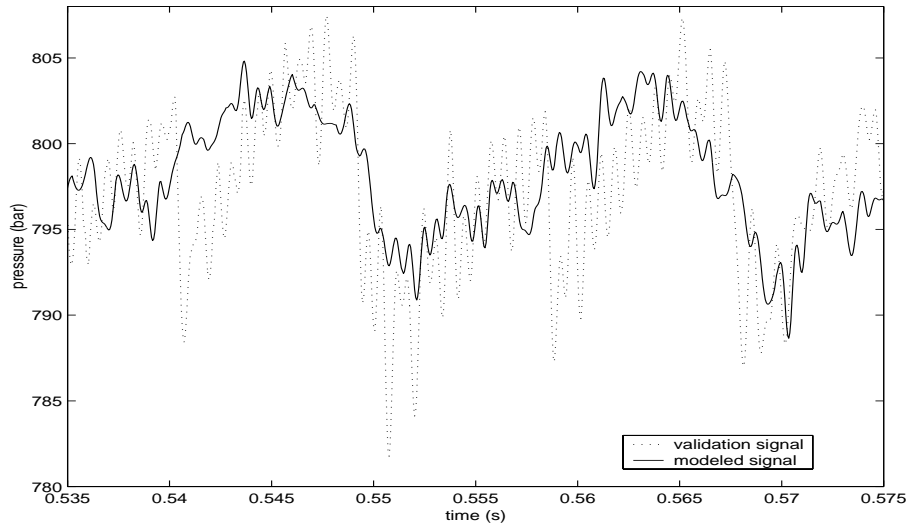


Figure 4.9: The modelled signal and the validation signal.

since the cluster is located near that frequency region. There are no other frequencies in the spectrum that possibly can derive from the oscillations in the injector signals apart from the cluster. Besides the frequencies around 800-900 bar that derive from the injectors, almost all the frequencies in the validation signal are found in the spectrum of the modelled signal. The amplitude of the frequency components do not always agree in the two spectra. This may depend on incorrectly estimated parameters and constants.

This modelling approach has served better as a way of developing the final model than as a proper modelling method itself. Therefore its results are not analysed as closely as the results derived from the model created by the wave equation method described in chapter 5. The problem that arose with the estimation of the parameters led to a decision which implied trying to model the system more accurately.

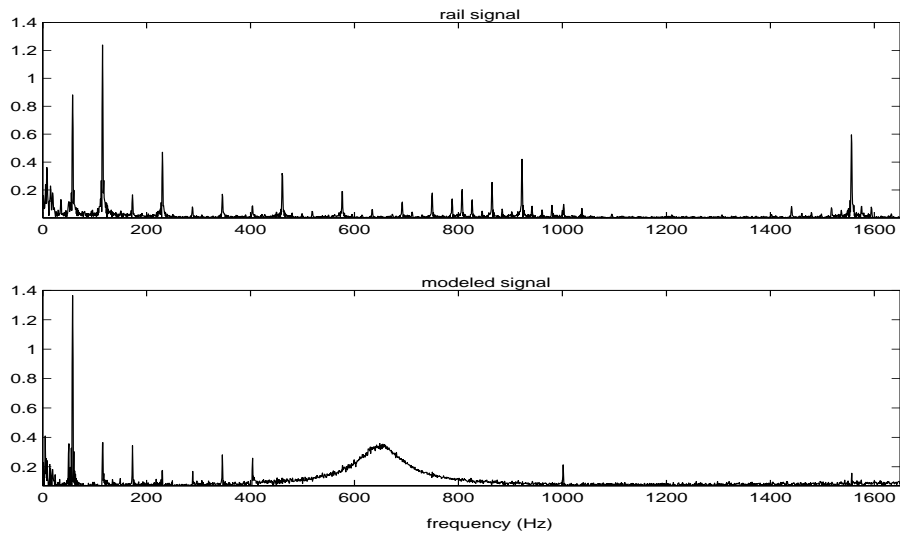


Figure 4.10: Frequency spectra of the modelled signal and the validation signal.

## 5 The Wave equation method

This modelling method is developed in order to explain the behaviour of the pressure waves more strictly than in the mass spring method.

### 5.1 The model

The model is developed from the general wave equation, which describes the propagation of waves in a medium. The particular equation that describes pressure waves is generated and then extended to serve this application. The model is lumped by making the wave equation discrete in a certain number of points along the rail. Pressure and time derivative of pressure in these points are chosen as states and boundary conditions are determined.

#### 5.1.1 The wave equation

In an idealistic case the propagation of pressure waves in one direction is described by the one-dimensional wave equation for pressure [9]

$$\frac{\partial^2 p}{\partial t^2} = c^2 \frac{\partial^2 p}{\partial x^2} \quad (5.1)$$

where  $p$  is pressure and  $c$  is the speed of the wave. In reality the wave is affected by energy losses from both the medium in which the wave is travelling and the conditions at the boundaries of the medium. Losses in the transmitting medium may be divided into three types: viscous losses, heat conduction losses and losses associated with molecular exchanges of energy. Unfortunately it is not possible to represent all the losses by a single modification of well established relations such as the wave equation. But according to [10], acoustic losses in many materials may be adequately described by a viscous damping term at room temperature. This is assumed to be applicable to the diesel engine fuel oil used in the CR System, even if the temperature at the working point the model is developed for is higher, i.e.  $40.5^\circ C$ . Therefore a wave equation which pays regard to the effects of viscous damping, will now be derived. The displacement from the equilibrium position of the atoms in a fluid is called  $\xi$ . By using this conception, pressure can be defined. If a pressure wave in a fluid is studied, consider a part between  $x$  and  $x + \Delta x$  in the medium. The mass of this element can be written as  $m = \rho A \Delta x$ , where  $\rho$  is the density of the fluid without a wave,  $A$  is the cross section area and  $\Delta x$  is the length of the element. Pressure

change is also defined as force  $F$  per area unit:

$$p(x) - p(x + \Delta x) = \frac{F}{A} \quad (5.2)$$

By using Newton's equation in order to express the force differently, following relation is developed

$$A(p(x) - p(x + \Delta x)) = \rho A \Delta x \frac{\partial^2 \xi}{\partial t^2} \quad (5.3)$$

which also can be written as:

$$\frac{p(x + \Delta x) - p(x)}{\Delta x} = -\rho \frac{\partial^2 \xi}{\partial t^2} \quad (5.4)$$

If  $\Delta x \rightarrow 0$  the expression will be:

$$\frac{\partial p}{\partial x} = -\rho \frac{\partial^2 \xi}{\partial t^2} \quad (5.5)$$

The absorption of energy from pressure waves in fluids is associated with a time lag of the condensation  $s$ , where  $s = -\frac{\partial \xi}{\partial x}$ , relative to the varying pressure  $p$ . This lag depends on the characteristic time required for

- Viscous stresses associated with relative fluid particle velocities to tend to equalize these velocities, or
- Heat conduction to occur between high pressure (high temperature) and low pressure (low temperature) regions or
- Molecular energy changes to occur

But as stated earlier, only the viscous losses are taken into consideration. In order to get the dissipation terms into the general wave equation, the time lag of the condensation  $s$  and the pressure fluctuations have to be described. Stokes developed the following equation for this purpose [11]

$$p = \rho c^2 s + R \frac{\partial s}{\partial t} \quad (5.6)$$

where  $\rho$  is the density of the medium and  $R = \frac{4}{3}\eta$  with  $\eta$  as the dynamic viscosity. By using the relation for the condensation  $s = -\frac{\partial \xi}{\partial x}$ , the force equation 5.5 and by taking the time derivative of the expression 5.6 twice, an extended version of the general wave equation can be found as:

$$\frac{\partial^2 p}{\partial t^2} = c^2 \frac{\partial^2 p}{\partial x^2} + \frac{R}{\rho} \frac{\partial^3 p}{\partial x^2 \partial t} \quad (5.7)$$

### 5.1.2 Lumping the states

The propagation of the pressure wave is now described by a partial differential equation. Now the states have to be chosen. A definition of the conception of states can be found in [8]:

The state of a system at a time  $t_0$  implies the amount of information that is needed to calculate an output  $y(t)$  for  $t > t_0$  if the input  $u(t)$  is given for  $t > t_0$

Since the wave equation is continuous the pressure at every point in the rail should be chosen as states. That would lead to an infinite number of states. The solution to this problem is to lump the state variables. This means that variables which are similar in character are combined to one state. This state will represent a mean value of the original states. For this model  $n$  number of points along the rail are considered to be important. This means that the infinite number of states can be reduced to states at these points. To be able to use the wave equation with a limited number of states, it has to be difference approximated in the space variable [12]. Both backwards and forwards difference approximation are used here.

$$\frac{\partial^2 p_i}{\partial x^2} = \frac{\frac{\partial p_{i+1}}{\Delta x} - \frac{\partial p_i}{\Delta x}}{\Delta x} = \frac{\frac{p_{i+1} - p_i}{\Delta x} - \frac{p_i - p_{i-1}}{\Delta x}}{\Delta x} = \frac{p_{i+1} - 2p_i + p_{i-1}}{(\Delta x)^2} \quad (5.8)$$

If this expression is inserted into the wave equation (5.7) there will be a discrete wave equation at each point along the rail that describes the state at that point.

$$\frac{\partial^2 p_i}{\partial t^2} = c^2 \frac{p_{i+1} - 2p_i + p_{i-1}}{(\Delta x)^2} - \frac{R}{\rho} \frac{\partial \left( \frac{p_{i+1} - 2p_i + p_{i-1}}{(\Delta x)^2} \right)}{\partial t} \quad (5.9)$$

This means that two states for each point are needed to describe the behaviour of the pressure wave in the rail, one for the pressure  $p_i$  and the second for the time derivative of the pressure  $\dot{p}_i$ :

$$x_j = p_i \quad (5.10)$$

$$x_{j+1} = \dot{p}_i \quad (5.11)$$

where  $i$  is an integer between 1 and  $n$  and  $j$  an integer between 1 and  $2n$ . The states will have the following form

$$\dot{x}_j = x_{j+1} \quad (5.12)$$

$$\dot{x}_{j+1} = \frac{c^2}{(\Delta x)^2}(x_{j+2} - 2x_j + x_{j-2}) - \frac{R}{\rho(\Delta x)^2}(x_{j+3} - 2x_{j+1} + x_{j-1}) \quad (5.13)$$

### 5.1.3 Boundary conditions

The wave equation describes the behaviour of a wave propagating undisturbed in a medium. To be able to model the pressure waves in the rail, the behaviour at the ends of the rail have to be taken into consideration.

The CR System is a complex system and the boundary conditions have to be determined as an approximation. The waves are assumed to be totally reflected at both ends of the rail. It is an approximation since there is a valve at one end of the rail where the waves loose energy and there may also be energy losses at the connections with the injection pipes and the pump pipe. Total reflection in a pipe with a closed end is shown in figure 5.1. The pressure at the two points closest to the ends will always have the same

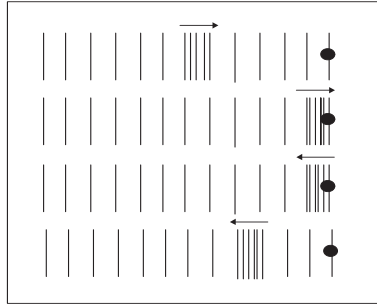


Figure 5.1: Reflection of an acoustic wave at a closed end of a tube.

pressure and pressure changes with regard to time, since reflection occurs without phase change [6]. That implies the following relations between the first four states and the four last states have the equivalent relations.

$$p_1 = p_2 \quad (5.14)$$

$$\dot{p}_1 = \dot{p}_2 \quad (5.15)$$

$$\begin{aligned} \ddot{p}_2 &= \frac{c^2}{(\Delta x)^2}(p_3 - 2p_2 + p_1) - \frac{R}{\rho(\Delta x)^2}(\dot{p}_3 - 2\dot{p}_2 + \dot{p}_1) = \\ &= \frac{c^2}{(\Delta x)^2}(p_3 - p_2) - \frac{R}{\rho(\Delta x)^2}(\dot{p}_3 - \dot{p}_2) \end{aligned} \quad (5.16)$$

### 5.1.4 State-space model

To be able to implement the model in SIMULINK, the system has to be written on state space form as follows

$$\dot{\mathbf{x}}(t) = \mathbf{A}\mathbf{x}(t) + \mathbf{B}\mathbf{u}(t) \quad (5.17)$$

$$\mathbf{y}(t) = \mathbf{C}\mathbf{x}(t) + \mathbf{D}\mathbf{u}(t) \quad (5.18)$$

where  $\mathbf{x}(t)$  are the states of the system,  $\mathbf{u}(t)$  are the inputs,  $\mathbf{y}(t)$  are the outputs and  $\mathbf{A}$ ,  $\mathbf{B}$ ,  $\mathbf{C}$  and  $\mathbf{D}$  are matrices. The equations developed from the extended wave equation will form the  $\mathbf{A}$  matrix, a system that describes the wave propagation. The  $\mathbf{B}$  matrix contains the inputs to the system, which are the time derivative of the pump signal and the injector signals. Because of the units in the state space model either the first time derivative or the second time derivative of the signals have to be used as inputs. The reason to chose the first derivative is that it is found more important to the model. When the time derivative of a signal is taken, higher frequencies will be amplified, since the derivative corresponds to a straight line (with slope 1) in the frequency domain. Consequently, these signals are lowpass filtered before they are used as inputs. As explained earlier, frequencies above 2000 Hz are considered as noise and therefore this frequency will be the cut-off frequency for these lowpass filters as well. As outputs the pressure at  $n$  points are chosen, and this is done in the  $\mathbf{C}$  matrix. The  $\mathbf{D}$  matrix contains only zeros since there are no direct terms in the system. The whole system will get the following general appearance:

$$\dot{\mathbf{x}}(t) = \begin{bmatrix} 0 & 1 & 0 & 0 & 0 & 0 & \dots & 0 & 0 & 0 & 0 & 0 & 0 \\ -C & -N & C & N & 0 & 0 & \dots & 0 & 0 & 0 & 0 & 0 & 0 \\ 0 & 0 & 0 & 1 & 0 & 0 & \dots & 0 & 0 & 0 & 0 & 0 & 0 \\ C & N & -2C & -2N & C & N & \dots & 0 & 0 & 0 & 0 & 0 & 0 \\ \vdots & \vdots & \vdots & \vdots & \vdots & \vdots & \ddots & \vdots & \vdots & \vdots & \vdots & \vdots & \vdots \\ 0 & 0 & 0 & 0 & 0 & 0 & \dots & 0 & 0 & 0 & 0 & 0 & 0 \\ 0 & 0 & 0 & 0 & 0 & 0 & \dots & C & N & -2C & -2N & C & N \\ 0 & 0 & 0 & 0 & 0 & 0 & \dots & 0 & 0 & 0 & 0 & 0 & 1 \\ 0 & 0 & 0 & 0 & 0 & 0 & \dots & 0 & 0 & C & N & -C & -N \end{bmatrix} \mathbf{x}(t) + \begin{bmatrix} 1 & 0 & 0 & \dots \\ 0 & 0 & 0 & \dots \\ 0 & 1 & 0 & \dots \\ 0 & 0 & 0 & \dots \\ 0 & 0 & 1 & \dots \\ 0 & 0 & 0 & \dots \\ \vdots & \vdots & \vdots & \ddots \end{bmatrix} \mathbf{u}(t)$$

$$\mathbf{y}(t) = \begin{bmatrix} 1 & 0 & 0 & 0 & 0 & \dots \\ 0 & 0 & 1 & 0 & 0 & \dots \\ 0 & 0 & 0 & 0 & 1 & \dots \\ 0 & 0 & 0 & 0 & 0 & \dots \\ \vdots & \vdots & \vdots & \vdots & \vdots & \ddots \end{bmatrix} \mathbf{x}(t)$$

$$\text{where } C = \frac{c^2}{(\Delta x)^2} \text{ and } N = \frac{R}{\rho(\Delta x)^2}.$$



### 5.1.5 Implementation

As a first try to model the system, the rail is divided into 17 parts, each approximately 3 cm long. This means that the model gets  $18 \cdot 2$  states and the positions for the pressure states are shown in figure 5.2. The physical parameters such as the compressibility constant, the viscosity and the density of the fuel are determined by using data for the certain working point found in [13] and [14]. The viscosity constant of the fuel is used as the  $\eta$  in the wave equation as a first assumption, but as explained earlier  $R$  (in equation 5.7) may serve as a damping constant for all acoustic losses in a material. This means that this constant may need to be increased to explained the real system. The state space model is implemented in SIMULINK.

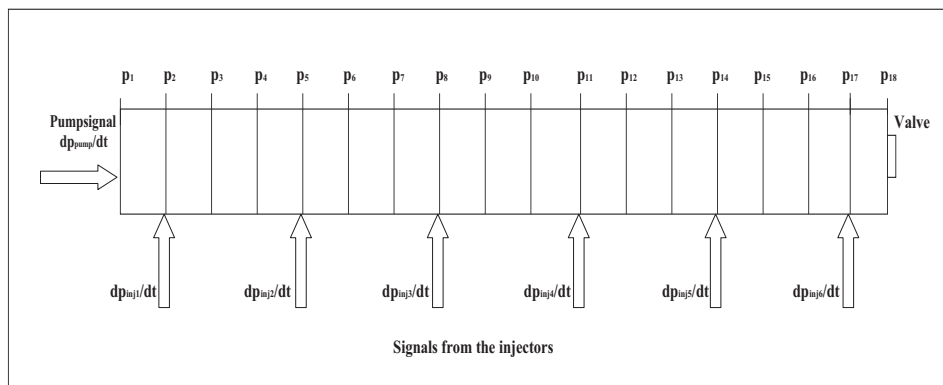


Figure 5.2: The model with inputs and outputs.

## 5.2 Analysis of the model

In this section the developed model will be examined and necessary improvements are discussed. If nothing else is mentioned the text refer to the working point the model is developed for (i.e. 2300 rpm, 800 bar,  $40.5^\circ C$ ).

### 5.2.1 Correction of energy absorption

When the model is simulated it becomes clear that at least one of the approximations is too optimistic. The simulation results show that the assumption that the whole acoustic wave is reflected at the ends of the rail does not agree completely with reality. The modelled waves reflect completely without any phase change or energy losses and accordingly a first order standing wave phenomenon arises. Since the rail is modelled

with closed ends, the node appears in the middle with two antinodes at the ends. In figure 5.3 it is possible to see the difference in the pressure signals at a point located at the end and a point located in the middle of the rail. In figure 5.4 the frequency spectra of the signals from figure 5.3 are shown. In section 3.3 the frequency of the first order standing wave in the rail is estimated to 1336 Hz. The frequencies around 1300 Hz in the spectrum for the p1 signal in figure 5.4 agree well with this frequency.

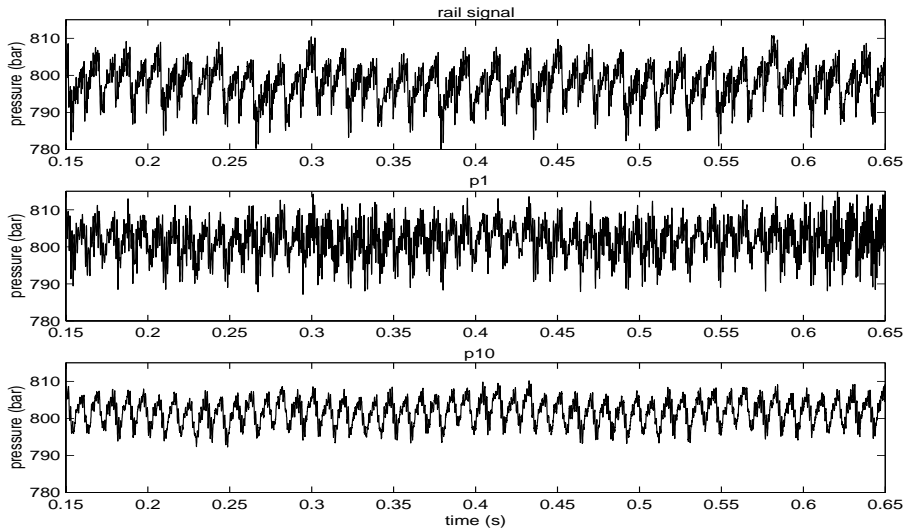


Figure 5.3: The validation signal and the modelled signals from positions at the end of the rail (p1) and in the middle (p10).

Even though the approximation in the boundary conditions seems too large, it is difficult to find relations that describe the actual conditions at the ends better. The pressure control valve is located at one end of the rail and the rail pressure sensor is placed at the other end. The sensor does not reflect the wave totally, but the reflection coefficient is not known. The valve does definitely not reflect the wave completely, but it is difficult to describe mathematically how much of the wave's energy that is absorbed. The reflection itself is also hard to describe since it changes due to the mean pressure. Energy is surely absorbed in the injection pipes too but as in the previous cases, it is difficult to know how much.

One solution to this problem may be to describe this energy absorption by other means. As explained in 5.1.1 the presence of viscosity leads to absorption of the wave's energy. The damping that comes from this phe-

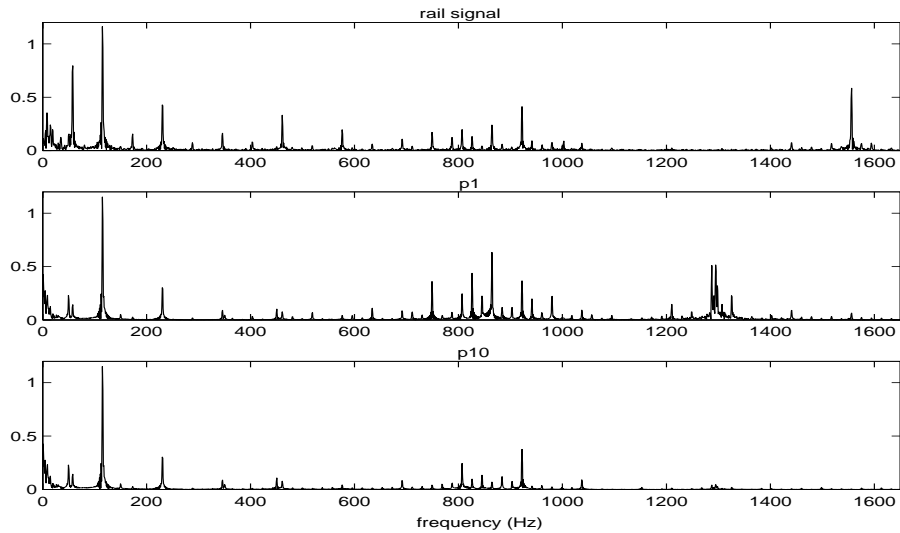


Figure 5.4: The frequency spectra of the rail signal and modelled signals from positions at the end of the rail (p1) and in the middle (p10).

nomena seems very tiny compared to the damping needed to explain the energy absorption at the ends. But still, in both cases it is a question of energy absorption. The idea is to let the damping of the wave at the ends be spread out in the medium by letting the  $R$  in the extended wave equation 5.3 refer to not only the viscosity but also to this extra damping. This new constant can be determined by simulating the model without injections and validating the model with another data-set than the one used in the final validation of the model. The pressure at points where injector pipes are connected to the rail are compared to measured data at the injectors. These signals are chosen since there are no other signals to use and the signals should be similar even if they have different locations. Both the time signals and the frequency spectra of the signals are used to develop the right value for the damping constant. The measured data set does not show any frequency components from the standing wave frequency region and this is used to estimate the constant. It is increased until these frequencies in the modelled data set disappear. When this is done the modelled signals get the appearance shown in figure 5.5. Figure 5.6 shows that the standing wave frequency at 1300 Hz is gone in the spectrum of the p1 pressure signal.

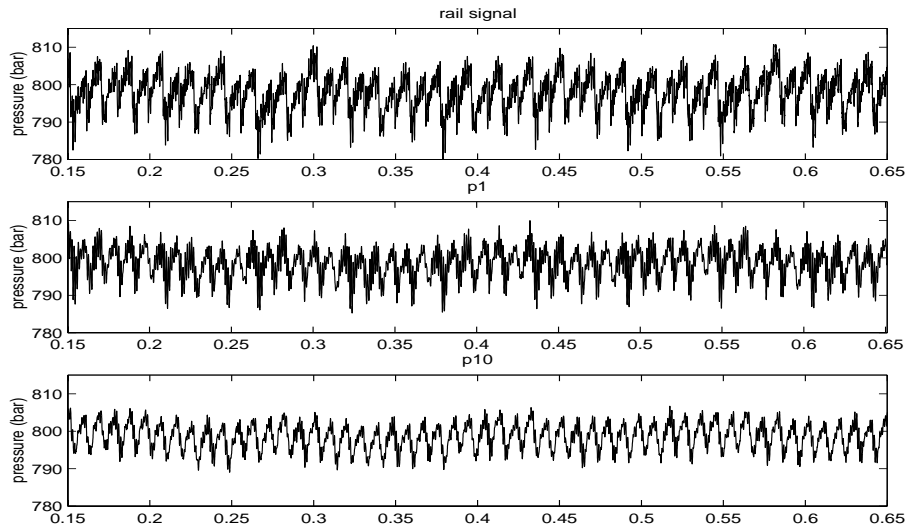


Figure 5.5: The validation signal and the modelled signals from positions at the end (p1) and in the middle (p10) of the rail after correction of the damping factor.

### 5.2.2 Results

When the correction of the damping factor is done the model seems to describe the real system much better (see figure 5.7). The principal features of the system seems to be described well by the model. The scaling of the modelled signal is not perfect, which may depend on the use of time derivatives as inputs. These signals are lowpass filtered before they are used which also means that they also become somewhat damped. Another reason to the scale deviation in the modelled signal may be that the pressure level of this signal is only determined by an initial value of the pressure state variable at this point. This is a result of using time derivatives as inputs, since these signals only describe the change in pressure (with regard to time).

If the frequency spectrum from the modelled signal is compared with the spectrum from the validation signal most of the frequencies agree (see figure 5.8). The difference in appearance between the two spectra shows in a sense the size of the model error. If the error is acceptable or not depends on what the model will be used for. Based on the model error in this case it can be assumed that the model is able to explain the main behaviour of the system, but reliable detailed information about the conditions in

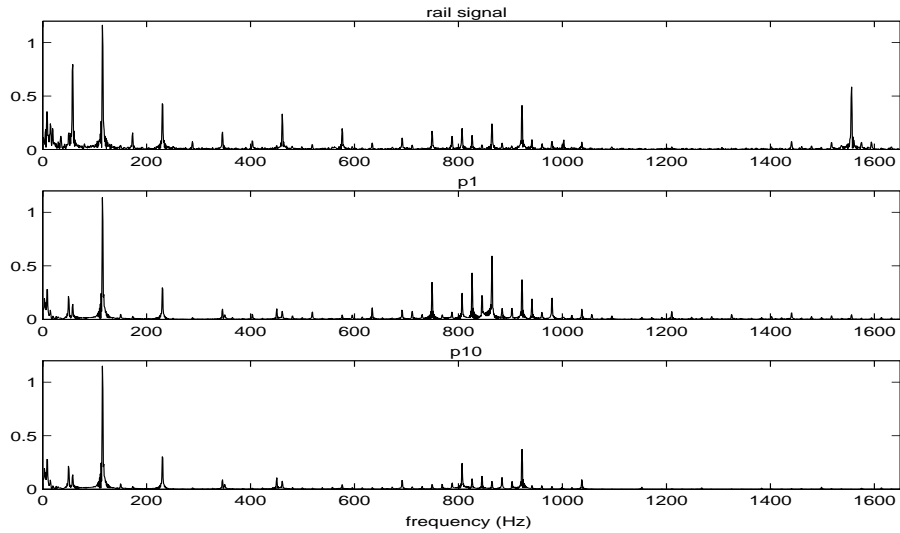


Figure 5.6: The frequency spectra of the rail signal and modelled signals from positions at the end (p1) and in the middle (p10) of the rail after correction of the damping factor.

the rail may not be available (see section 5.2.4). The frequencies coming from the damped oscillations in the injections, i.e. around 800-1200 Hz, do not agree completely. This may depend on the use of the same injection signal for all the inputs corresponding to the injections (see section 3.2). In reality the damped oscillations in the injection signals have slightly different frequencies, which also results in a different frequency spectrum. Some frequency amplitudes in the modelled signal are not as intense as in the rail signal. This depends partially on the damping caused by the filtering of the input signals. The main frequency of the pump (i.e. 57 Hz) for instance, does not get the desired amplitude in the spectrum of the modelled signal. The amplitude of the 1555 Hz frequency component is unfortunately not so high, which indicates that the cause of this peak is not modelled correctly. As explained in section 3.3 it is uncertain where this frequency component comes from, which makes it even more difficult to improve the model. Other frequencies in the rail signal that do not appear at all in the modelled signal are the 4th (575 Hz) and the 5th (690 Hz) multiple of the main frequency from the injections.

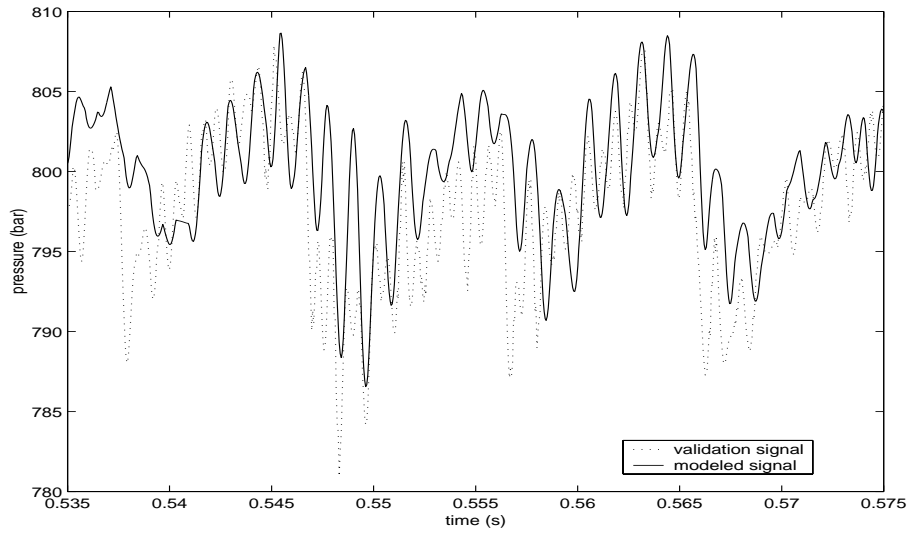


Figure 5.7: The modelled signal with the validation signal.

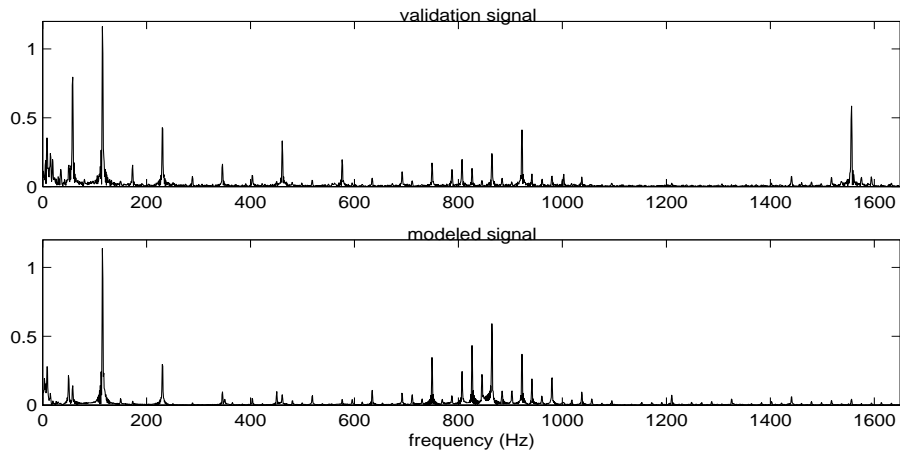


Figure 5.8: Frequency spectra of the validation signal and the modelled signal.

### 5.2.3 Domain of validity

The model is developed for a working point with a mean pressure of 800 bar, an engine speed of 2300 rpm and a temperature of  $40.5^{\circ}\text{C}$ . To examine how well the model describes the real system at other working points, the model is simulated with data sets shown in table 5.1 as inputs. The reason

Data set	Pressure level [bar]	Engine speed [rpm]	Temperature [C]
A	500	2300	40.5°
B	1200	2300	40.5°
C	800	1000	40.5°
D	800	3200	40.5°

Table 5.1: Working points

for not examine working points where the temperature is changed is that the results of changing this parameter was found insignificant in a previous study of this system [3]. The results are presented in figure 5.9. The model seems to work better for the working points represented by data sets B and C than for the other two working points. The model seems to work quite poorly for the working point corresponding to data set A. The modelled signal and the validation signal differ a lot sometimes. This may not only depend on the model but also the fact that the signals used as inputs and validation signals are not recorded in phase. This is compensated with time delays as accurately as possible, but the right phase is difficult to find in some signals. This problem implies that the signals can not be guaranteed to be in phase. The only solution to this problem is to record new data sets where the signals are in phase. An obvious difference between the modelled signal and the validation signal in all cases is the pressure level. The general appearance of the modelled signals agree quite well with the validation signals, but the mean level of the signals differ for every examined working point in figure 5.9. This may also depend on that the validation signal and the modelled signal are not in phase.

#### 5.2.4 The purpose of the model

The model is developed for diagnosis purposes and in order to find the cause of the earlier discussed engine problems. The first aim can be considered to be achieved since the model shows satisfactory results. There are no other expressed requirements for the model that have to be fulfilled yet. To find out if the model also answers the second purpose, a further study has to be done. In the following section of this chapter, it is declared how the model can be used to find out more about what happens in the rail. Since the model is developed for a certain working point, an explanation of how a model for the critical working points can be generated is given in chapter 6.

The differences in the measured pressure signals from the injectors are shown in figure 5.10. The most obvious deviation is that the peaks caused

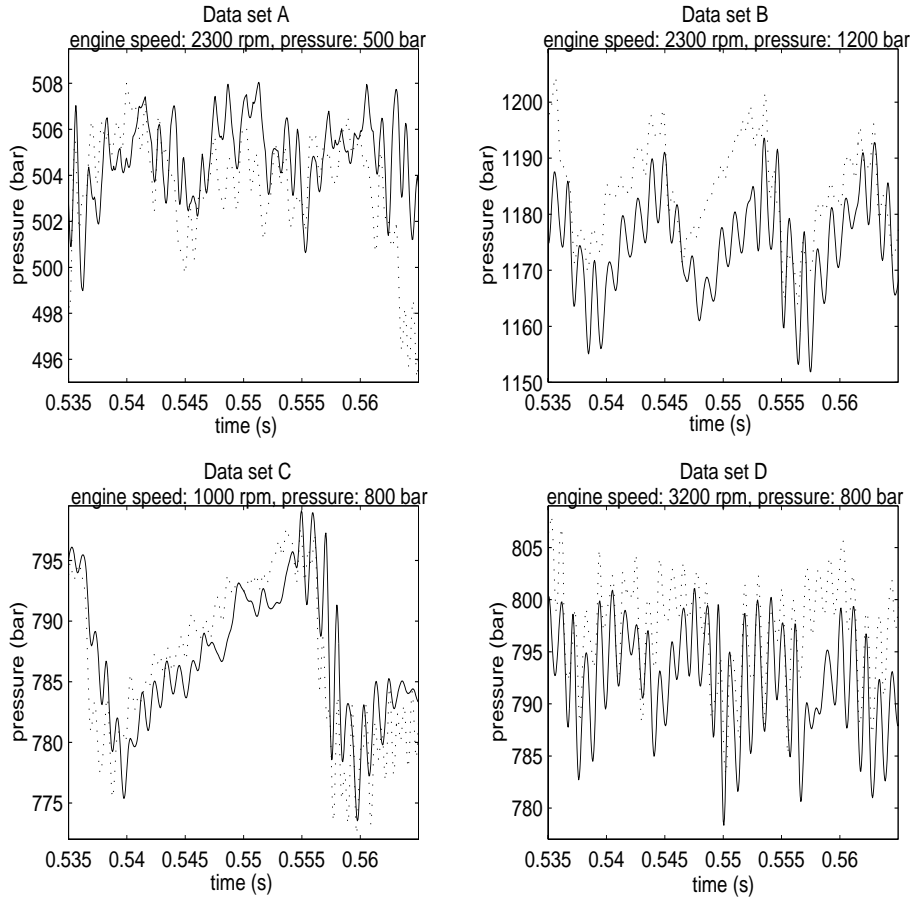


Figure 5.9: The modelled signals (solid lines) with the validation signals (dotted lines).

by the injections vary a lot in amplitude among the injectors. The amplitude of these peaks in injector signal 1 is only two thirds of the other's amplitude levels. These signals can be compared with the modelled signals at the points along the rail that correspond to the connection with the injection pipes (i.e. p2, p5, p14 and p17 as figure 5.2 shows). The difference in amplitude is not as obvious among the modelled signals as among the measured signals. If the signals are examined in detail it is possible to find a tiny difference in amplitude. The first (p2) and the last (p17) signal have both an amplitude that is approximately 1 bar larger than the second signal (p5). The third signal (p14) has an amplitude that is about 5 bar less than



the second signal. Apart from this no deviation of interest is found. This means that the deviation among the signals found in the measured data set is not created by the model. But for this working point the engines are running smoothly. A similar study would anyhow be of interest for the working points where the engine problems occur.

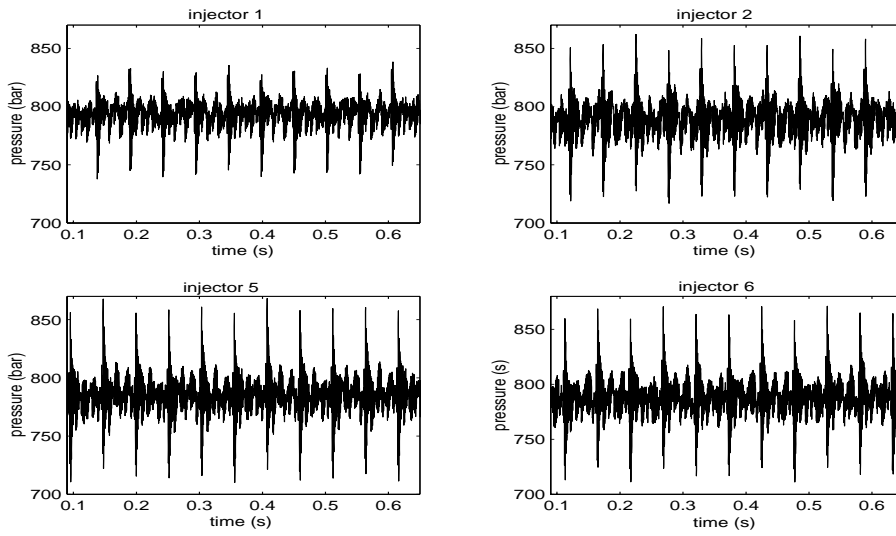


Figure 5.10: Measured signals at injector 1,2,5 and 6.

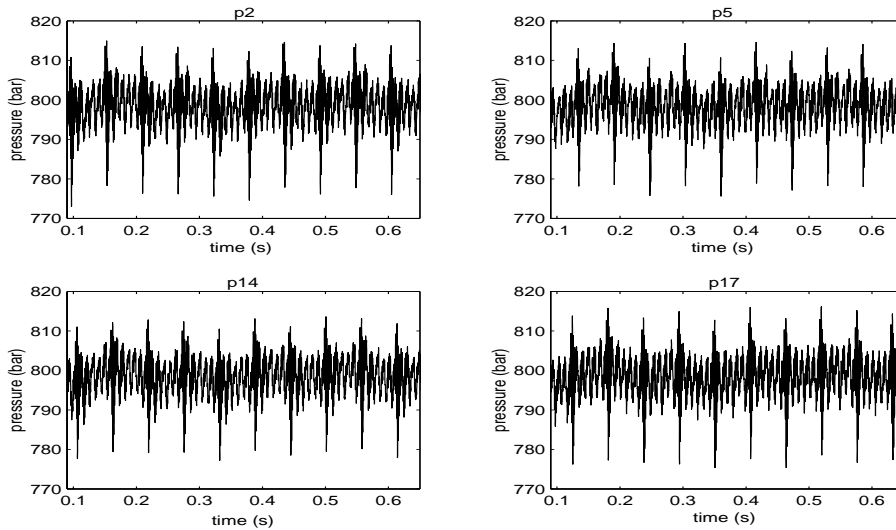


Figure 5.11: Modelled signals: p2, p5, p14 and p17.

## 6 An extension of the model

The physical parameters in the model vary a lot due to the working conditions for the system. The pressure varies between approximately 300 and 1350 bar, the engine speed ranges from 700 rpm to 3200 rpm and the temperature varies between 40 and 120 °C. Parameters in the model such as the density and the compressibility constant depend among others on pressure and temperature. This means that the developed model from chapter 5 can not be expected to work well for all working conditions of the system. As shown in section 5.2.3 the model does not describe the system as properly at these conditions as at the working point it was developed for. When the model is used for examining the behaviour of the pressure in the rail it is preferable to develop new models and adapt them to the current conditions instead of using the first model for all working points.

### 6.1 Implementation

The development of the new models are done by using the model from chapter 5 as a base structure. Then only the parameters that depend on the change of the working point are modified. For these calculations hydraulic oil is used instead of diesel engine fuel oil. The reason is that the physical properties of the fluids are similar but more data can be found for the latter one. According to [13] the change in the compressibility constant  $K$  and the density  $\rho$  due to changes in pressure and temperature can be described in the following manner:

$$K(p) = \frac{1}{\frac{a}{10} - \frac{b}{10}\left(\frac{p-p_0}{10}\right) + \frac{c}{10}\left(\frac{p-p_0}{10}\right)^2} \quad (6.1)$$

$$\rho(p, T) = \rho_0 \cdot e^{(a\left(\frac{p-p_0}{10}\right) - \frac{b}{2}\left(\frac{p-p_0}{10}\right)^2 + \frac{c}{3}\left(\frac{p-p_0}{10}\right)^2 - \beta_T \cdot T)} \quad (6.2)$$

where  $\beta_T$  is the coefficient of volume expansion (approximately constant in this case),  $T$  is the temperature,  $\rho_0$  is the density of a fluid at a reference pressure  $p_0$  of 130 bar and  $a$ ,  $b$  and  $c$  are constants<sup>3</sup>. Relations 6.1 and 6.2 are developed to describe measured data for the hydraulic oil. The adaptation of parameters answering to the working point is done automatically by MATLAB functions when the data sets of the current working point are chosen. The m-file where this is done can be found in appendix B. The opening of the pressure control valve changes due to the mean pressure. This is not taken into consideration since the available information about

<sup>3</sup> $a=7.4e^{-4}$ ,  $b=3.6e^{-6}$  and  $c=1.2e^{-8}$

Data set	Pressure level [bar]	Engine speed [rpm]	Temperature [C]
A	500	2300	40.5°
B	1200	2300	40.5°
C	800	1000	40.5°
D	800	3200	40.5°

Table 6.1: Working points

the behaviour of the valve is deficient. To ignore this change is considered to be a better approximation to the real system than to make a correction of the model based on the available information.

## 6.2 Results

Models for the working points shown in table 6.1 are developed to find out how well the model structure works. The same working points are chosen as in the analysis of the validity domain of the first model (see section 5.2.3). This is done in order to be able to compare the results. The results from the simulations are presented in figure 6.1. The models manage to show the most important features of the system in all cases. But if the results are compared it seems like the models for working points B and C describe the system better than the two other models. The incongruity in the models for working points A and D may depend on that the signals are not in phase as discussed in section 5.2.3. Anyhow, it can be easily established that these models show better results than if the first model is used for all working points, by comparing figure 5.9 and figure 6.1.

## 6.3 The purpose of the model

A model that explains the problems with the engines that arise at certain working conditions, is not found yet since the exact working points are not known. But as soon as this information becomes clear the current physical parameters can be inserted in the developed model structure and a model for that working point is generated. This model has to be validated by using the rail signal for this working point and it is not until then that it can be stated if this purpose of the model is served.

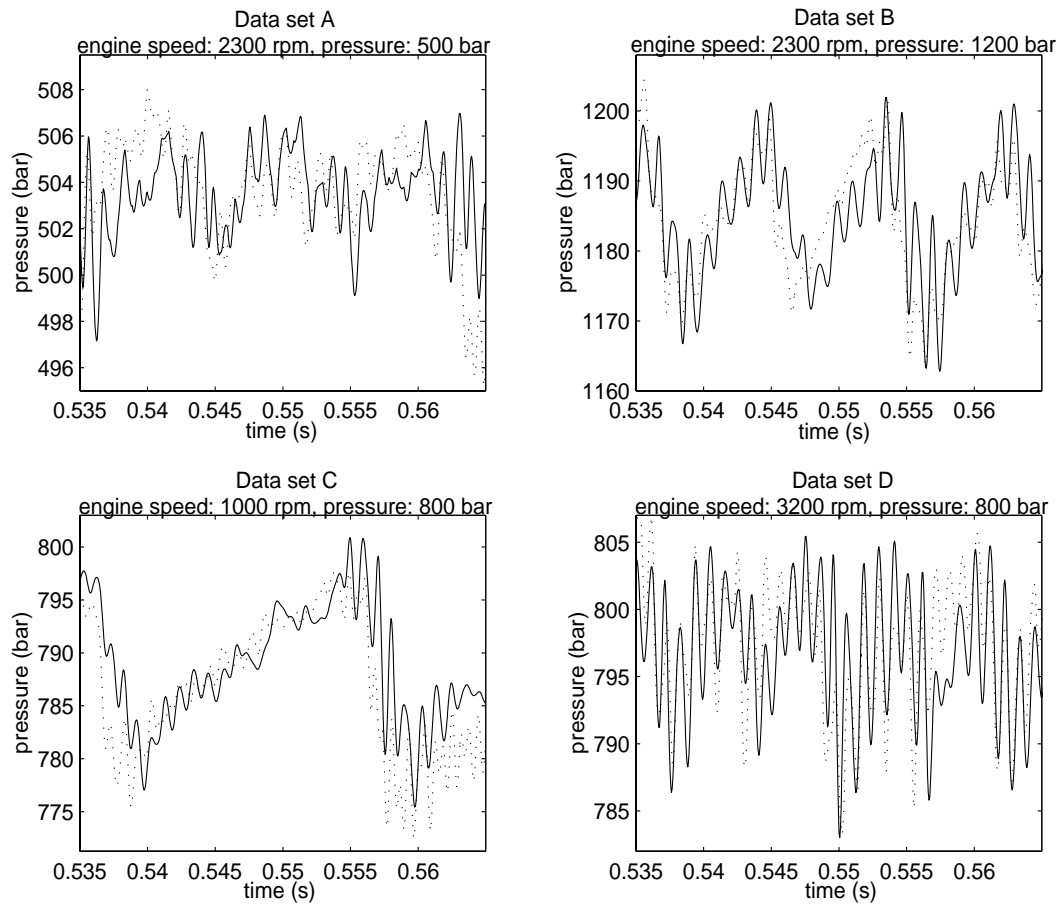


Figure 6.1: The modelled signal (solid lines) with the validation signal (dotted lines).

## 7 Conclusions and recommendations

Two different models of the pressure waves in the CR System are developed. Both are based on well known physical relations. The first modelling approach implies approximating the real system with a mechanical system and then modelling the mechanical waves. The second method describes the pressure waves in the system by using an extended wave equation and then by making the system discrete. The first approach seems to be too much of an approximation. Many parameters have to be roughly estimated and the idea of using another physical system makes it also hard to understand the model and the results. The approach served well as a manner to learn more about the system though. The latter approach describes the system more strictly, which makes this method preferable. Simulation results show that the final model manages to create the principal features of the system. The aim of this study was to describe the behaviour of the pressure in the system, which can be considered to be achieved since the results are satisfactory. Consequently the first object of the model itself is also served, to create a model that can be used as a part of a larger model for diagnosis purposes. But the main purpose of the model is to find the cause of the engine problems at certain working conditions. Since the exact conditions are not known yet, a first model is developed for a working point in the middle of the operational domain. When the physical parameters corresponding to the critical working conditions are found, these can easily be inserted into the generated model structure. Not until then can it be established if the model answers this purpose.

### 7.1 Recommended improvements

The approximation of the boundary conditions was too optimistic and therefore viscous damping in the rail have to explain the energy absorption that occurs at the ends of the rail. A further developed model may describe this absorption more properly by using other boundary conditions. But to be able to do that more information about the ends of the rail is needed. The function of the pressure control valve has to be clear and also the reflection rate at the ends. The filtering of the time derivative of the input signals is of great importance to the model. The filter that is used in the present model is a very simple lowpass filter. Since the model is very sensitive to changes in the filter, an implementation of a more advanced filter such as butterworth filter or chebyshev filter, may improve of the model. To be completely sure of the results produced by the model, it is recommended to record new sets

of data where the signals are in phase. Anyhow this would facilitate the use of the model. For using the model in the present condition, the signals do first have to be synchronized before any simulation is possible, which is very time-consuming. Another way of improving the accuracy of the model is to divide the rail into more numerous discrete parts when the states are lumped (see section 5.1.2).

---

## References

- [1] The MathWorks Inc. *Using Simulink*, 1999.
- [2] Bosch. Motorsteuerung für dieselmotoren, common rail system für pkw. CD-ROM, 1998. Stuttgart, Germany.
- [3] Michael Froehlich. Einspritzmengenbestimmungen am common-rail-einspritzsystem durch druckverlaufsanalyse mittels neuronaler netze. Master's thesis, University of Tübingen, faculty of informatics, 1996.
- [4] John A. Roberson and Clayton T. Crowe. *Engineering Fluid Mechanics*. Houghton Mifflin, Boston, USA, 1975. ISBN: 0-395-18607-2.
- [5] The MathWorks Inc. *Using Matlab*, 1997.
- [6] Richard E. Berg and David G. Stork. *The physics of sound*. Prentice Hall, Englewood Cliffs, N.J., USA, 2nd edition, 1995. ISBN: 0-13-183047-3.
- [7] Herbert John Pain. *The physics of Vibrations and Waves*. John Wiley and Sons, Chichester , Great Britain, 4th edition, 1993. ISBN: 0-471-93619-7.
- [8] Lennart Ljung and Torkel Glad. *Modellbygge och simulering*. Studentlitteratur, Lund, Sweden, 1991. ISBN: 91-44-31871-5.
- [9] K. Uno Ingard. *Fundamentals of Waves and Oscillations*. Cambridge University Press, Cambridge , Great Britain, 1988. ISBN: 0-521-32734-2.
- [10] Bertram A. Auld. *Acoustic Fields and waves in solids*. John Wiley and Sons, New York, USA, 1973. ISBN: 0-471-03702-8.
- [11] Lawrence E. Kinsler. *Fundamentals of acoustics*. John Wiley and Sons, New York, USA, 2nd edition, 1967. ISBN: 0-471-48049-5.
- [12] Otto Föllinger. *Regelungstechnik: Einführung in die Methoden und ihre Anwendung*. Hüthig, Heidelberg , Germany, 8th edition, 1994. ISBN 3-7785-2336-8.
- [13] Juan Luis Hernandez Carabias. Hydraulische vorgänge des common-rail-einspritzsystems. Daimler-Benz AG, Stuttgart, Germany, 1996.

- [14] Mayo D Hersey. Viscosity of diesel engine fuel oil under pressure. Technical Report No. 315, The National Aeronautics and Space Act, NACA (now NASA), Washington, USA, 1929.



## Appendix A: Mass spring method

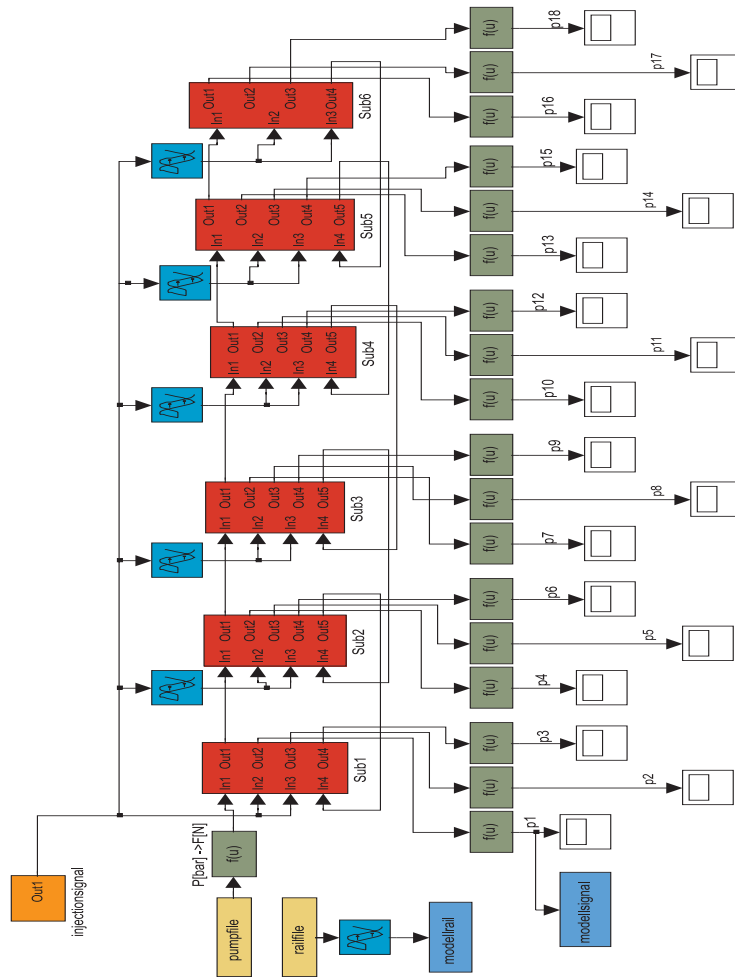


Figure A.1: The model implemented in SIMULINK.

```

m=0.0021103278 % mass
constant=10e10; % constant used in the transformation of forces into pressures
k=4.905332037e6 % spring constant
b=150; % damping constant
m1=m; m2=m; m3=m; b1=b; b2=b; b3=b; k1=k; k2=k; k3=k;
% State-space model for the first part of the rail
A1=[-b1/m1 -1/m1 b1/m1 0 0 0;
     k1 0 -k1 0 0 0;
     b1/m2 1/m2 -(b1+b2)/m2 -1/m2 b2/m2 0;
     0 0 k2 0 -k2 0;
     0 0 b2/m3 1/m3 -(b2+b3)/m3 -1/m3;
     0 0 0 0 k3 0];
B1=[1/m1 0 0 0;
     0 0 0 0;
     0 -1/m2 0 0;
     0 0 0 0;
     0 0 1/m3 b3/m3;
     0 0 0 -k3];
C1=[0 0 0 0 b3 1;
     0 1 0 0 0 0;
     0 0 0 1 0 0;
     0 0 0 0 0 1];
D1=[0 0 0 -b3;
     0 0 0 0;
     0 0 0 0;
     0 0 0 0];
%State-space model for the second part of the rail
m4=m; m5=m; m6=m; b4=b; b5=b; b6=b; k4=k; k5=k; k6=k;
A2=[-b4/m4 -1/m4 b4/m4 0 0 0;
     k4 0 -k4 0 0 0;
     b4/m5 1/m5 -(b4+b5)/m5 -1/m5 b5/m5 0;
     0 0 k5 0 -k5 0;
     0 0 b5/m6 1/m6 -(b5+b6)/m6 -1/m6;
     0 0 0 0 k6 0];
B2=[1/m4 0 0 0;
     0 0 0 0;
     0 -1/m5 0 0;
     0 0 0 0;
     0 0 1/m6 b6/m6;
     0 0 0 -k6];
C2=[0 0 0 0 b5 1;
     0 1 0 0 0 0;
     0 0 0 1 0 0;
     0 0 0 0 0 1;
     1 0 0 0 0 0];
D2=[0 0 0 -b6;
     0 0 0 0;
     0 0 0 0;
     0 0 0 0];
% State-space model for the third part of the rail
m7=m; m8=m; m9=m; b7=b; b8=b; b9=b; k7=k; k8=k; k9=k;
A3=[-b7/m7 -1/m7 b7/m7 0 0 0;
     k7 0 -k7 0 0 0;
     b7/m8 1/m8 -(b7+b8)/m8 -1/m8 b8/m8 0;
     0 0 k8 0 -k8 0;
     0 0 b8/m9 1/m9 -(b8+b9)/m9 -1/m9;
     0 0 0 0 k9 0];
B3=[1/m7 0 0 0;
     0 0 0 0;
     0 -1/m8 0 0;
     0 0 0 0;
     0 0 1/m9 b9/m9;
     0 0 0 -k9];
C3=[0 0 0 0 b8 1;
     0 1 0 0 0 0;
     0 0 0 1 0 0;
     0 0 0 0 0 1;
     1 0 0 0 0 0];
D3=[0 0 0 -b9;
     0 0 0 0;
     0 0 0 0;
     0 0 0 0];

```

```

% State-space model for the fourth part of the rail
m10=m; m11=m; m12=m; b10=b; b11=b; b12=b; k10=k; k11=k; k12=k;
A4=[-b10/m10 -1/m10 b10/m10 0 0 0;
     k10 0 -k10 0 0 0;
     b10/m11 1/m11 -(b10+b11)/m11 -1/m11 b11/m11 0;
     0 0 k11 0 -k11 0;
     0 0 b11/m12 1/m12 -(b11+b12)/m12 -1/m12;
     0 0 0 0 k12 0];
B4=[1/m10 0 0 0;
     0 0 0 0;
     0 -1/m11 0 0;
     0 0 0 0;
     0 0 1/m12 b12/m12;
     0 0 0 -k12];
C4=[0 0 0 0 b11 1;
     0 1 0 0 0 0;
     0 0 0 1 0 0;
     0 0 0 0 0 1;
     1 0 0 0 0 0];
D4=[0 0 0 -b12;
     0 0 0 0;
     0 0 0 0;
     0 0 0 0];
% State-space model for the fifth part of the rail
m13=m; m14=m; m15=m; b13=b; b14=b; b15=b; k13=k; k14=k; k15=k;
A5=[-b13/m13 -1/m13 b13/m13 0 0 0;
     k13 0 -k13 0 0 0;
     b13/m14 1/m14 -(b13+b14)/m14 -1/m14 b14/m14 0;
     0 0 k14 0 -k14 0;
     0 0 b14/m15 1/m15 -(b14+b15)/m15 -1/m15;
     0 0 0 0 k15 0];
B5=[1/m13 0 0 0;
     0 0 0 0;
     0 -1/m14 0 0;
     0 0 0 0;
     0 0 1/m15 b15/m15;
     0 0 0 -k15];
C5=[0 0 0 0 b14 1;
     0 1 0 0 0 0;
     0 0 0 1 0 0;
     0 0 0 0 0 1;
     1 0 0 0 0 0];
D5=[0 0 0 -b15;
     0 0 0 0;
     0 0 0 0;
     0 0 0 0];
% State-space model for the sixth part of the rail, a terminating wall
m16=m; m17=m; m18=m; b16=b; b17=b; b18=b; k16=k; k17=k; k18=k;
A6=[-b16/m16 -1/m16 b16/m16 0 0 0;
     k16 0 -k16 0 0 0;
     b16/m17 1/m17 -(b16+b17)/m17 -1/m17 b17/m17 0;
     0 0 k17 0 -k17 0;
     0 0 b17/m18 1/m18 -(b17+b18)/m18 -1/m18;
     0 0 0 0 k18 0];
B6=[1/m16 0 0 0;
     0 0 0 0;
     0 -1/m17 0 0;
     0 0 0 0;
     0 0 1/m18 -1/m18;
     0 0 0 0];
C6=[0 1 0 0 0 0;
     0 0 0 1 0 0;
     0 0 0 0 0 1;
     1 0 0 0 0 0];
D6=[0 0 0 0;
     0 0 0 0;
     0 0 0 0;
     0 0 0 0];

```

Figure A.2: The m-file where the physical parameters and the state space model are defined.

## Appendix B: Wave equation method

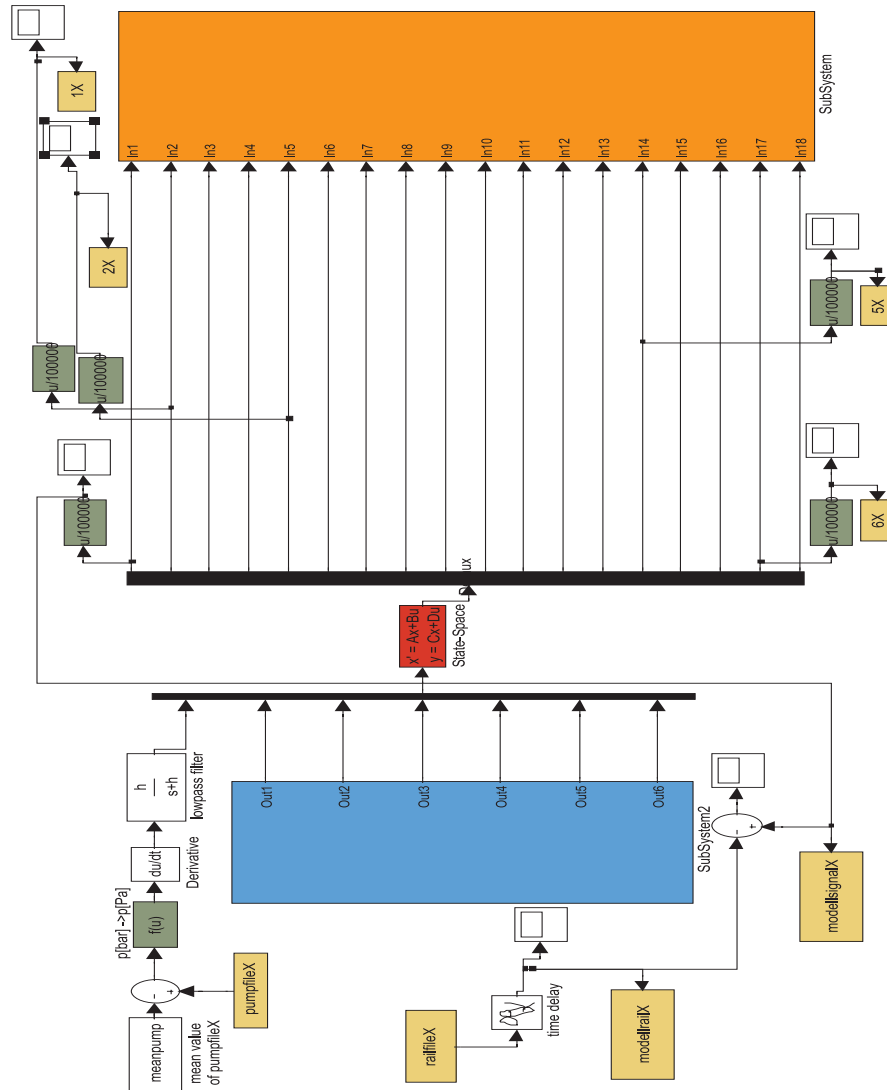


Figure B.1: The model implemented in SIMULINK.





## Appendix C: Evaluation of the models in MATLAB

```
%to compare the the frequency spectra of the modeled signal and the validation signal
figure
subplot(2,1,1)
load modellrailX
m=(ans)';
m=(m(:,2)-mean(m(:,2)));
m0 = [m ;zeros(length(m),1)];
f=(1/20000)*abs(fft(m0));
plot((0:length(f)-1)/length(f)/(1/20000),f,'b')
subplot(2,1,2)
load modellsignalX
m=(ans)';
m=(m(:,2)-mean(m(:,2)));
m0 = [m ;zeros(length(m),1)];
f=(1/20000)*abs(fft(m0));
plot((0:length(f)-1)/length(f)/(1/20000),f,'b')

%to compare the modeled signal and the validation signal
figure
load modellrailX
m=(ans)';
m=m(:,2);
y=resample(m,13108,length(m)');
plot(time,y,'g')
hold on
load modellsignalX
n=(ans)';
n=n(:,2);
x=resample(n,13108,length(n)');
plot(time,x,'b')
```

Figure C.1: The most important MATLAB code used to examine signals.